Applied Mathematical Modelling 128 (2024) 1–25

Contents lists available at ScienceDirect

Applied Mathematical Modelling

journal homepage: www.elsevier.com/locate/apm

# Catenary configuration and geometric stiffness matrix of inextensible cables: Analytical high-order asymptotic solutions for parametric design

Marco Lepidi [a,b,*]

[a] DICCA - Department of Civil, Chemical and Environmental Engineering, University of Genova, Genova, Italy
[b] INFN - National Institute for Nuclear Physics - Genova Section, Genova, Italy

ARTICLE INFO

*Keywords:*
Cable structures
Inclined cable
Closed-form solution
Asymptotic techniques
Perturbation methods
Direct stiffness method
Parametric design

ABSTRACT

The analytical and geometric study of catenary curves is a classic matter of applied mathematical modeling. The paper systematizes a methodological strategy to achieve fully analytical solutions for the mechanical problem of determining the equilibrium configuration assumed by inextensible inclined cables under gravitational loads. By developing a two-step perturbation scheme, the statically indeterminate equilibrium problem is asymptotically formulated, and asymptotic solutions are obtained in the form of convergent polynomial series of terms with increasing orders of smallness. As a major achievement, the asymptotic analytical solutions are explicit functions of the governing parameters and automatically satisfy the integral compatibility condition, which traditionally requires a numerical solution to assess the hyperstatic unknowns. The mathematical conditions for the existence of admissible solutions and asymptotic consistency of the perturbation scheme are provided, while the characteristic properties of the asymptotic series are recognized or demonstrated. Parametric analyses successfully verify the high approximation accuracy achievable by high-order asymptotic series, truncated to a large but finite number of terms. With the aim of extending the methodology to the largest possible variety of cable structure applications, a fully analytical, although asymptotic, expression of the geometric stiffness matrix of inextensible inclined cables is determined. Parametric analyses confirm that high-order asymptotic expressions can accurately approximate the exact stiffness matrix assessed numerically. This achievement opens up viable opportunities for analytically studying and parametrically designing complex cable structures (including collaborations with other structural elements), within the framework of the direct stiffness method. Finally, the feasibility and effectiveness of the asymptotic direct stiffness method are successfully verified by solving in a fully-analytical way a paradigmatic static problem for the catenary cable-stayed beam.

## 1. Introduction

Owing to the successful combination of extreme lightness, high strength and fine parametric designability, cable structures are considered unparalleled mechanical solutions for covering medium and large spans. By exploiting the limitless possibilities of

* Correspondence to: DICCA - Department of Civil, Chemical and Environmental Engineering, University of Genova, Genova, Italy.
*E-mail address:* marco.lepidi@unige.it.

https://doi.org/10.1016/j.apm.2023.12.019
Received 16 August 2023; Received in revised form 6 November 2023; Accepted 18 December 2023

Available online 2 January 2024

morphological shaping, the unprecedented perspectives opened by high-performing materials and the synergistic collaborations with other structural elements (beams, arches, rings), cables are profitably used in countless applications, including – among the others – suspension bridges, cable-stayed roofs, transmission infrastructures, mooring lines, guyed masts, sail rigging, tethered vehicles, robot manipulators. In this regard, there are few scientific subjects in which a centuries-old uninterrupted tradition of physical-mathematical developments, dating back to pioneering works by Leonardo da Vinci and Galileo Galilei about funicular polygons and curves, have had and continue to have as many and equally fruitful applications in such a wide variety of traditional and emerging fields of applied mathematics, engineering and technology. Therefore, it is not surprising that numerous scientific publications and monographs in recent decades have been focused on the theoretical fundamentals and modern developments of the topic, with particular attention to the rich scenario of static and dynamic phenomena that can characterize the mechanical behavior of horizontal or inclined cables [1–4].

Searching for the equilibrium configuration assumed by a suspended cable hanging between fixed supports can be regarded as a statically indeterminate shape-finding problem. Starting from the end of the seventeenth century, when the problem was posed as a mathematical contest by Jacob Bernoulli, the topic has attracted the interest of many outstanding mathematicians, including Leibniz, Euler, Huygens, Johann Bernoulli and many others [5,6]. Specifically, if the ideal hypothesis of axial indeformability is introduced, the curved configuration assumed by a perfectly flexible cable under self-weight is known to be mathematically described by a transcendental (non-polynomial) function, whose map in the vertical (gravitational) plane is referred to as *catenary* curve [1,5]. Admitting elastic axial deformability determines a slightly different configurational curve, mathematically described by a distinct transcendental function, analytically expressible in cartesian parametric form, whose map is known as *elastic catenary* curve [1]. Both configurational functions parametrically depend on the horizontal component of the axial tension (equal to the horizontal reaction at the supports), playing the role of hyperstatic unknown, which has to be numerically determined a posteriori by solving nonlinear compatibility equations, expressing the indeformability constraint (for the catenary), or a pair of coupled boundary conditions (for the elastic catenary). Therefore, apart from some particular applications in which the cable tension can be independently assigned as a control variable, the systematic need to numerically address a fundamental part of the solution process (sometimes resorting to iterative procedures) suggests to consider the catenary functions as *quasi-analytical* solutions.

The scientific relevance of the matter is not limited to the geometric problem itself, but involves many complementary mechanical problems that use the static equilibrium configuration as reference. In the linear and nonlinear dynamics of prestressed curved continua, among the other fields, the axial tension and curvature may determine significant hardening or softening effects. Within this challenging framework, mathematical complexities in the algebraic and differential treatment of transcendental functions have inevitably led to the proliferation of approximate – yet analytical – static solutions, mainly of the polynomial type (quadratic, cubic and related low-degree spline functions). Nonetheless, approximating the catenary functions does not modify the indeterminate nature of the mechanical problem; thus, fully analytical solutions of the compatibility equations are seldom available and are mostly limited to low-order approximations [1]. On the other hand, numerous studies have shown that the highest possible accuracy in the description of the static cable configuration, even if approximate, is a crucial aspect in direct and inverse mechanical problems, including – for instance – the assessment of the linearized modal properties [7–9], the description of nonlinear interactions and aerodynamic phenomena [10–14], the evaluation of damage and temperature effects [15,16], the performance of active control strategies [17,18] and the reliability of identification procedures [19,20]. Therefore, the search for analytical solutions that properly balance the opposing requirements of mathematical tractability and physical accuracy remains an open question that is worthy of investigation. From the application viewpoint, a renewed and decisive impulse in this direction is also given by the growing demand for explicit formulas in the emerging fields of parametric design and reverse engineering.

Based to this motivating scenario, the present paper proposes *fully-analytical* solutions for the asymptotic expression of the *quasi-analytical* catenary function that characterizes the static response of an inextensible cable to self-weight. The primary objective is to by-pass the algorithmic bottleneck represented by the numerical assessment of the hyperstatic unknown, by achieving an analytical – although asymptotic – solution, expressible as fully parametric function of the mechanical data. This mathematical achievement is pursued by means of a suited perturbation technique that – as minor character of novelty – does not require to order a priori the smallness of the known parameters. The drawbacks inherent in the approximate nature of the solution are balanced by the possibility to achieve the desired convergence by extending the asymptotic solution to high orders. As complementary objective, a decisive step towards the systematic application of the asymptotic strategy to complex cable nets and cable structures is provided by determining the equivalent of the elastic stiffness matrix for the inextensible cable, in the quasi-analytical catenary form as well as in the fully-analytical asymptotic form.

The paper is organized in two parts. First, the quasi-static problem related to inclined inextensible cables is formulated (Section 2). The exact quasi-analytical catenary solutions are briefly recalled (Subsection 2.1), and the perturbation strategy to achieve fully-analytical asymptotic solutions is described (Subsection 2.2). A comparison is carried out in terms of hyperstatic unknowns. Second, the geometric stiffness matrix of the inclined inextensible cable is determined (Section 3). The exact quasi-analytical stiffness matrix is presented (Subsection 3.1), and its fully analytical asymptotic expression is determined (Subsection 3.2). A comparison is carried out in terms of stiffness coefficients. Finally, the paradigmatic static problem for the catenary cable-stayed beam if formulated (Section 4). The exact numerical solution is achieved by formulating a hybrid displacement-force method (Subsection 4.1), while an high-order analytical approximation of the solution is provided by employing an asymptotic direct stiffness method (Subsection 4.2).

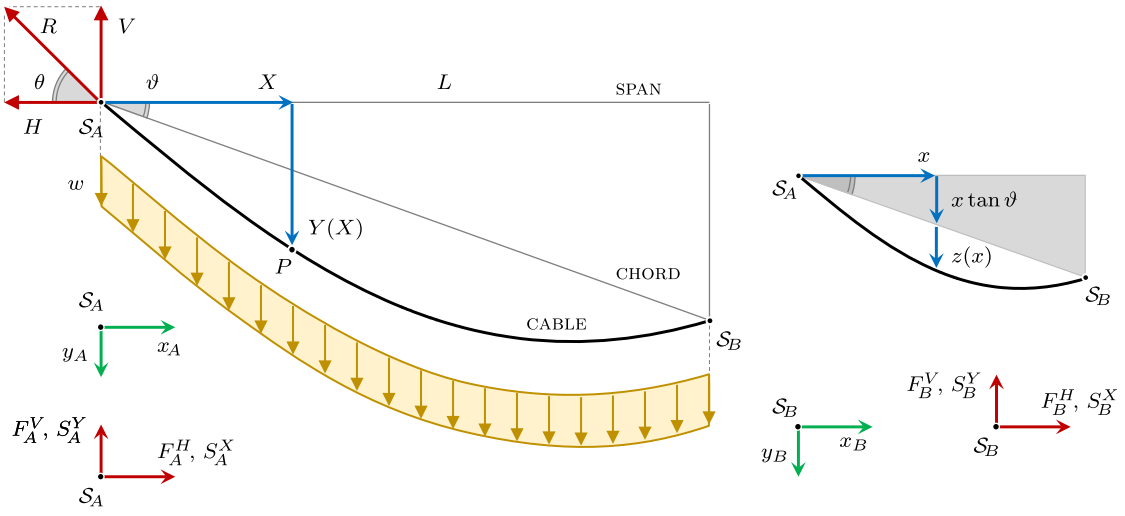


**Fig. 1.** Catenary configuration of the inclined cable hanging between fixed support under self-weight.

## 2. Static equilibrium problem

According to a classic mechanical formulation, an inextensible suspended cable can be described as a one-dimensional non-polar continuum [1,2]. The continuum is assumed homogeneous and perfectly flexible in the transversal directions. Based on these assumptions, the structural properties of the cable are the self-weight density $w$ and the natural length $L_0$. The cable tension $N$ is an axial force of reactive nature, due to the constraint of axial inextensibility, and is required to be locally collinear to the equilibrium configuration, due to the absence of shear and flexural rigidities. Consequently, searching the cable response under gravity loads consists in solving a geometric shape-finding problem, pursuing proper descriptors of the unknown curvilinear configuration $\mathcal{C}_S$ satisfying the equilibrium in the vertical plane (Fig. 1). The cable is supposed hanging between two fixed supports $\mathcal{S}_A$ and $\mathcal{S}_B$. Cables hanging between supports at different levels (*inclined* cables) are characterized by a *span* length $L$ (horizontal inter-support distance) that differs from the *chord* length $L\sec\vartheta$ (inter-support distance), due to positive *inclination angles* $\vartheta$.

### 2.1. Catenary solutions

Considering a cartesian coordinate system with origin coincident with the support $\mathcal{S}_A$, the equilibrium configuration assumed by the inextensible cable in the vertical plane is described by the unknown configurational function $Y(X)$.[1] The axial tension $N(X)$, the horizontal reaction $H$ and vertical reaction $V$ at the support $\mathcal{S}_A$ are also unknown. The problem can be classified as statically indeterminate. Imposing the horizontal equilibrium of the generic infinitesimal cable element implies that the horizontal component of the axial tension is a constant, coincident with the reaction $H$. By employing this result in the equation ruling the vertical equilibrium, the configurational function $Y(X)$ is governed by the so-called *funicular* equation

$$\frac{d^2Y}{dX^2} = -\frac{w}{H}\left[1+\left(\frac{dY}{dX}\right)^2\right]^{1/2} \tag{1}$$

where the coefficient $w/H$ is constant but partially unknown, because the horizontal reaction $H$ plays the role of hyperstatic unknown, to be determined a posteriori by imposing a *compatibility condition*, according to a solution strategy resembling the classical force method used to solve statically indeterminate elastic problems. The equation is complemented by the boundary conditions $Y(0)=0$ and $Y(L)=L\tan\vartheta$.

The differential problem can be expressed in nondimensional form by introducing dimensionless variables, together with a minimal set of independent dimensionless parameters, sufficient to fully characterize the mechanical system. To this purpose, the cable span $L$ and the horizontal reaction $H$ can be selected as reference (known) length and (unknown) force, so that the dimensionless quantities

$$x=\frac{X}{L},\qquad y=\frac{Y}{L},\qquad \delta=\frac{wL_0}{8H},\qquad \Lambda=\frac{L_0}{L}\cos\vartheta \tag{2}$$

are defined. The fully geometric parameter $\Lambda$ is known as *aspect ratio* and represents the ratio between the natural cable length and the chord length $L\sec\vartheta$. The fundamental parameter $\delta$ expresses the ratio between the approximate cable weight $wL\sec\vartheta$ and the

[1] Here the variable nomenclature and positive signs preserve the conventions adopted in the pivotal monograph by Irvine [1].

approximate chord-aligned reaction $H \sec\vartheta$. Both parameters are positive by definition. The nondimensional form of the governing equation reads

$$y'' = -\delta \left[1 + \left(y'\right)^2\right]^{1/2} \tag{3}$$

where the apex indicates differentiation with respect to the dimensionless independent variable $x \in [0,1]$. The role of dimensionless hyperstatic unknown is assumed by the parameter $\delta$. The equation is complemented by the boundary conditions $y(0) = 0$ and $y(1) = \tan\vartheta$. Recalling the properties of hyperbolic function, the exact solution is the well-known *catenary* function

$$y_c(x) = \frac{\sinh(4\delta x)\sinh(\Psi_c - 4\delta x)}{4\delta}, \qquad \Psi_c = 4\delta + \operatorname{arcsinh}\left(\frac{4\delta\tan\vartheta}{\sinh(4\delta)}\right) \tag{4}$$

where the quantity $\Psi_c$ can be physically interpreted as the arc whose hyperbolic sine is the tangent of the angle $\theta$ (with $\theta > \vartheta$) between the catenary curve (at the support $S_A$) and the horizontal line. Consequently, the relation $\sinh(\Psi_c) = \tan\theta = \nu/h$ (referred to as *hyperstatic relation* in the following) holds.

The hyperstatic unknown $\delta$ is univocally assessed a posteriori, in order to identify the unique geometrically compatible solution among all the statically determinable catenary functions $y_c(x)$. The compatibility condition expresses the geometric requirement that the $\delta$-dependent arc-length of the catenary curve equates the natural length of the cable (*compatibility equation*), to respect the inextensibility. In nondimensional form, the compatibility equation reads $\Lambda_c = \Lambda$, where the arc-length of the catenary curve is

$$\Lambda_c = \cos\vartheta \int_0^1 \left[1 + \left(y_c'\right)^2\right]^{\frac{1}{2}} \mathrm{d}x = \frac{\cos\vartheta}{8\delta}\left[\sinh(\Psi_c) - \sinh\left(\Psi_c - 8\delta\right)\right] \tag{5}$$

according to differential geometry. Consequently, the compatibility condition imposes a nonlinear (transcendental) equation that requires to be solved numerically for the unknown $\delta$. Naturally, an admissible (real positive) solution exists only if the natural length of the cable exceeds the inter-support distance. Therefore, the compatibility condition is subordinated to the *admissibility inequality* $\Lambda > 1$.

Once the catenary solution is analytically determined and the hyperstatic unknown is numerically assessed, the other quantities of interest completing the solution of the mechanical problem are

$$h = \frac{\cos\vartheta}{4\Lambda\delta}, \qquad \nu = \frac{\cos\vartheta}{4\Lambda\delta}\sinh(\Psi_c), \qquad n(x) = \frac{\cos\vartheta}{4\delta\Lambda}\cosh\left[4\delta(1-2x) + \operatorname{arcsinh}\left(\frac{4\delta\tan\vartheta}{\sinh(4\delta)}\right)\right] \tag{6}$$

where $h = 2H/(wL_0)$ and $\nu = 2V/(wL_0)$ are the dimensionless horizontal and vertical reactions at support $S_A$, respectively, while $n(x) = 2N/(wL_0)$ is the dimensionless axial force at the abscissa $x$.

### 2.2. Asymptotic solutions

A feasible mathematical alternative to exact (quasi-analytical) catenary solutions can be provided by fully analytical – although expressed in asymptotic form – solutions, achievable by means of perturbation techniques. Perturbation techniques are powerful asymptotic methods that are widely used in a large variety of scientific research fields, ranging from direct problems concerning linear and nonlinear dynamics, stability and bifurcation [21–23] to inverse problems dealing with modal identification, optimal spectral design, damping and damage detection [24–26]. Perturbation methods are also classical and well-established strategies to study different problems in cable mechanics, including static behaviors [27,28], linear and nonlinear dynamic phenomena [2,29,30], aerodynamic instabilities [14,31], active vibration control [32,33].

A few preliminary considerations are required to anchor the perturbation strategy to a solid physical ground. The leading idea is that, due to their typical lightness (small $w$) and high tensioning (large $H$), structural cables tend to be characterized by geometric closeness between the static equilibrium configuration and the inter-support chord. According to a classic nomenclature, this geometric property is commonly referred to as cable *shallowness*. Consequently, the static problem for shallow cables can be reformulated by introducing the change of dimensionless variables

$$y(x) = y_0(x) + z(x) = x\tan\vartheta + z(x) \tag{7}$$

where the linear function $y_0(x) = x\tan\vartheta$ describes the inclined chord between the supports (Fig. 1), while the new configuration variable $z(x)$ describes the small dip of the static cable profile below the chord [1]. Applying the change of variable and without any approximation, equation (3) becomes

$$z'' = -8\delta\left[1 + \tan^2\vartheta + 2\tan\vartheta\, z' + \left(z'\right)^2\right]^{1/2} \tag{8}$$

while the boundary conditions become $z(0) = 0$ and $z(1) = 0$. The primary objective of the perturbation strategy is to pursue a fully analytical solution, expressed as explicit parametric function of the assigned mechanical data (that is, the aspect ratio $\Lambda$ and inclination angle $\vartheta$).

Following a standard multi-parametric perturbation scheme, the unknown solution $z(x)$ is postulated to be expressible as an asymptotically convergent series of $n$ terms $z_i(x)$, scaled by increasing integer powers of a small dimensionless bookkeeping parameter $\epsilon \ll 1$. The series reads

$$z_{[n]}(x) = \sum_{i=1}^{n} \epsilon^i \, z_i(x) = \epsilon \, z_1(x) + \epsilon^2 z_2(x) + ... + \epsilon^i z_i(x) + ... + \epsilon^n z_n(x) \tag{9}$$

where all the functions $z_i(x)$ work as independent unknown configurational variables. The function $z_i(x)$ can be also referred to as $i$-th *configurational sensitivity*. To complete the mathematical formulation of the perturbation problem, the hyperstatic unknown $\delta$ can be considered small by hypothesis, coherently with the assumption of cable shallowness. Therefore, the ordering

$$\delta_{[n]} = \epsilon\delta_1 + \epsilon^2\delta_2 + ... + \epsilon^i\delta_i + ... + \epsilon^n\delta_n \tag{10}$$

can be assumed. The independent unknowns $\delta_i$ will be referred to as *hyperstatic coefficients* in the following.

Solving the perturbation problem requires to assess all the hyperstatic coefficients $\delta_i$ necessary to define the configurational sensitivity functions $z_i(x)$ for $i = 1, ..., n$. Therefore, the bookkeeping parameter can be fully reabsorbed. The $n$-th order solution $z_{[n]}(x)$ is expected to asymptotically tend to the exact solution for growing $n$-values (increasing *approximation orders*). Indeed, in mathematical form, truncating the series at a finite number $n$ of terms implies a certain approximation in the description of the exact configuration, with residual difference belonging to the order $\mathcal{O}(\epsilon^{n+1})$. As minor peculiarity with respect to other perturbation approaches for the statics of inclined shallow cables, it can be noted that the ordering postulated a priori by equations (9)-(10) concerns only unknown quantities, whereas the ordering of the data (aspect ratio $\Lambda$) is introduced only a posteriori, for consistency reasons.

By substituting the variable expansion (9) and the parameter ordering (10) in equation (8), expanding and collecting terms of the same $\epsilon$-power, an ordered hierarchical system of linear *perturbation equilibrium equations* is obtained. By considering orders up to and including the sixth ($n = 6$), the system reads

$$\epsilon^1 : \quad z_1'' = -8\delta_1 \sec\vartheta \tag{11}$$

$$\epsilon^2 : \quad z_2'' = -8\delta_2 \sec\vartheta - 8\delta_1 \sin\vartheta z_1' \tag{12}$$

$$\epsilon^3 : \quad z_3'' = -8\delta_3 \sec\vartheta - 8\left[\delta_1 z_2' + \delta_2 z_1'\right] \sin\vartheta - 4\delta_1 (z_1')^2 \cos^3\vartheta \tag{13}$$

$$\epsilon^4 : \quad z_4'' = -8\delta_4 \sec\vartheta - 8\left[\delta_1 z_3' + \delta_2 z_2' + \delta_3 z_1'\right] \sin\vartheta + \\ - 4\left[2\delta_1 z_1' z_2' + \delta_2 (z_1')^2\right] \cos^3\vartheta + 4\delta_1 (z_1')^3 \sin\vartheta \cos^4\vartheta \tag{14}$$

$$\epsilon^5 : \quad z_5'' = -8\delta_5 \sec\vartheta - 8\left[\delta_1 z_4' + \delta_2 z_3' + \delta_3 z_2' + \delta_4 z_1'\right] \sin\vartheta + \\ - 4\left[\delta_1 (z_2')^2 + 2\delta_1 z_1' z_3' + 2\delta_2 z_1' z_2' + \delta_3 (z_1')^2\right] \cos^3\vartheta + \\ + 4\left[3\delta_1 (z_1')^2 z_2' + \delta_2 (z_1')^3\right] \sin\vartheta \cos^4\vartheta + \delta_1 (z_1')^4 \cos^5\vartheta (1 - 5\sin^2\vartheta) \tag{15}$$

$$\epsilon^6 : \quad z_6'' = -8\delta_6 \sec\vartheta - 8\left[\delta_1 z_5' + \delta_2 z_4' + \delta_3 z_3' + \delta_4 z_2' + \delta_5 z_1'\right] \sin\vartheta + \\ - 4\left[2\delta_1 z_2' z_3' + \delta_2 (z_2')^2 + 2\delta_2 z_1' z_3' + 2\delta_3 z_1' z_2' + 2\delta_1 z_1' z_4' + \delta_4 (z_1')^2\right] \cos^3\vartheta + \\ + 4\left[3\delta_1 z_1' (z_2')^2 + 3\delta_1 (z_1')^2 z_3' + 3\delta_2 (z_1')^2 z_2' + \delta_3 (z_1')^3\right] \sin\vartheta \cos^4\vartheta + \\ + \left[\delta_2 (z_1')^4 + 4\delta_1 z_2' (z_1')^3\right] \cos^5\vartheta \left(1 - 5\sin^2\vartheta\right) - \delta_1 (z_1')^5 \cos^6\vartheta \sin\vartheta \left(3 - 7\sin^2\vartheta\right) \tag{16}$$

while homogeneous boundary conditions $z_i(0) = 0$ and $z_i(1) = 0$ must be imposed at each order. Clearly, the hierarchy of perturbation equations can be extended to higher orders ($n > 6$), if necessary for the sake of solution accuracy. As a complementary remark, it might be worth noting that including the effects of elastic cable extensibility, which are fully describable by the small dimensionless geometric-to-elastic stiffness ratio $H/EA = \epsilon^m \mu$ (where $EA$ indicates the axial cable rigidity), would enrich the right-hand term of perturbation equations at all the orders $\epsilon^i$ with $i \geq m$.

The system solutions can be obtained straightforwardly by attacking the equations in cascade, starting from the lowest order, returning the *generating solution* $z_1(x)$. Thereafter (for $i > 1$), the $i$-th perturbation order $\epsilon^i$ systematically states an ordinary differential non-homogeneous linear equation involving only the second derivative of the $i$-th unknown variables $z_i(x)$ – at the left hand – and a known polynomial term, involving the first derivatives of all the lower-order variables – at the right hand. Since the generating solution is a second $x$-degree (quadratic) function, the higher $\epsilon$-order solutions must be polynomials of increasing $x$-degrees (cubic, quartic, quintic,...). Specifically, after integration and imposition of the boundary conditions, the solution of the $i$-th order (power of the perturbation parameter $\epsilon$) is a polynomial function including terms up to the $(i+1)$-th degree (power of the variable $x$), reading

$$\epsilon^i : \quad z_i(x) = \sum_{j=0}^{i+1} c_{ij} x^j = c_{i1} x + c_{i2} x^2 + ... + c_{i(i+1)} x^{i+1} \tag{17}$$

where the coefficients $c_{ij}$ – here not reported for the sake of synthesis – can be demonstrated to generally depend on all the unknown hyperstatic coefficients $\delta_k$ (with $k \leq i$). As a minor mechanical remark, the lowest-order approximation of the cable *sag* (dip at

midspan $x = 1/2$) reads $y_1(1/2) = \delta_1 \sec\vartheta$, meaning that the dominant part $\delta_1$ of the quantity $\delta$ can be interpreted as the *sag-to-span ratio* of the parabolic cable characterized by a certain aspect ratio $\Lambda$, suspended between leveled supports ($\vartheta = 0$).

The hyperstatic coefficients $\delta_i$ must be univocally assessed a posteriori, in order to identify the unique geometrically compatible solution among all the statically determinable polynomial functions $y_{[n]}(x)$, satisfying the perturbation equilibrium equations. The compatibility equation $\Lambda_p = \Lambda$ requires that the arc-length $\Lambda_p$ of the *polynomial* curve equates the natural length of the cable, to respect the inextensibility. First, the change-of-variable (7) is introduced in the integral expression of the nondimensional arc-length. Second, the configurational function $z(x)$ is replaced by its asymptotic expression $z_{[n]}(x)$, yielding

$$\Lambda_p = \cos\vartheta \int_0^1 \left[1 + \tan^2\vartheta + 2\tan\vartheta\, z'_{[n]} + \left(z'_{[n]}\right)^2\right]^{1/2} \mathrm{d}x \tag{18}$$

which depends on all the hyperstatic coefficients $\delta_i$. By operating coherently with the perturbation scheme, the length $\Lambda_p$ can be asymptotically expressed in the form $\Lambda_{p[n]} = \Lambda_{p0} + \epsilon\,\Lambda_{p1} + \epsilon^2\Lambda_{p2} + ... + \epsilon^i\Lambda_{pi} + ... + \epsilon^n\Lambda_{pn}$, where the lowest-order series terms are $\Lambda_{p0} = 1$ and $\Lambda_{p1} = 0$, while the high-order terms read

$$\Lambda_{p2} = \tfrac{8}{3}\delta_1^2\cos^2\vartheta \tag{19}$$

$$\Lambda_{p3} = \tfrac{16}{3}\delta_1\delta_2\cos^2\vartheta \tag{20}$$

$$\Lambda_{p4} = \left[\tfrac{8}{3}\delta_2^2 + \tfrac{16}{3}\delta_1\delta_3 + \tfrac{32}{45}\delta_1^4\,A_0(\vartheta)\right]\cos^2\vartheta \tag{21}$$

$$\Lambda_{p5} = \left[\tfrac{16}{3}\delta_1\delta_4 + \tfrac{16}{3}\delta_2\delta_3 + \tfrac{128}{45}\delta_1^3\delta_2\,A_0(\vartheta)\right]\cos^2\vartheta \tag{22}$$

$$\Lambda_{p6} = \left[\tfrac{8}{3}\delta_3^2 + \tfrac{16}{3}\delta_2\delta_4 + \tfrac{16}{3}\delta_1\delta_5 + \tfrac{64}{15}\delta_1^2\delta_2^2\,A_0(\vartheta) + \tfrac{128}{45}\delta_1^3\delta_3\,A_0(\vartheta) + \tfrac{256}{945}\delta_1^6\,B_0(\vartheta)\right]\cos^2\vartheta \tag{23}$$

where the zero-th order auxiliary quantities $A_0(\vartheta) = 8 - 5\cos^2\vartheta$ and $B_0(\vartheta) = 35\cos^4\vartheta - 56\cos^2\vartheta + 24$ have been introduced. From the viewpoint of the perturbation strategy, it is important to remark that the arc-length $\Lambda_{p[n]}$ depends on all the hyperstatic coefficients $\delta_i$ up to $i = n - 1$.

To briefly recap, determining the static equilibrium configuration requires (i) to assign the inclination angle $\vartheta$ and the aspect ratio $\Lambda$, and (ii) to enforce the compatibility equation $\Lambda_p = \Lambda$, to be solved in the hyperstatic unknown $\delta$. The assigned aspect ratio must satisfy the *admissibility inequality* $\Lambda > 1$. Within the framework of the perturbation strategy – however – the postulate of cable shallowness (expressed by $\delta \in \mathcal{O}(\epsilon)$ in the ordering of equation (10)) can be respected only if the assigned aspect ratio $\Lambda$ satisfies the additional requirement $\Lambda = 1 + \mathcal{O}(\epsilon^2)$, consistently with the asymptotic result for the arc-length $\Lambda_p = 1 + \mathcal{O}(\epsilon^2)$. This fundamental requirement is inherent to the perturbation strategy and will be conventionally referred to as the *consistency condition* in the following. The consistency is automatically verified if the aspect ratio can be ordered as $\Lambda = 1 + \epsilon^2\Lambda_2$, where $\Lambda_2$ represents the natural extra-length to be assigned as mechanical parameter. From the physical viewpoint, these mathematical considerations formalize the intuitive concept that the natural length of inextensible but shallow cables must be greater (inextensibility condition), but not much greater (shallowness postulate) than the distance between the supports.

Once the aspect ratio has been consistently ordered, the inextensibility condition $\Lambda_p = \Lambda$ can be imposed in the asymptotic form $\Lambda_{p[n]} = 1 + \epsilon^2\Lambda_2$. Therefore, collecting terms of the same $\epsilon$-order, an ordered hierarchy of algebraic *perturbation compatibility equations* in the unknown hyperstatic coefficients is stated. The perturbation equations non identically satisfied return the solutions

$$\delta_1 = \frac{\Lambda_1}{4\cos\vartheta} \tag{24}$$

$$\delta_3 = \frac{\Lambda_1\Lambda_2}{16\cos\vartheta} - \frac{\Lambda_1\Lambda_2}{10\cos^3\vartheta} \tag{25}$$

$$\delta_5 = -\frac{\Lambda_1\Lambda_2^2}{128\cos\vartheta} - \frac{3\Lambda_1\Lambda_2^2}{40\cos^3\vartheta} + \frac{17\Lambda_1\Lambda_2^2}{175\cos^5\vartheta} \tag{26}$$

where auxiliary known quantity $\Lambda_1 = (6\Lambda_2)^{1/2}$ has been introduced to simplify the notation. It is worth remarking that the even coefficients $\delta_2, \delta_4, ...$ are systematically null (meaning that the alternative ordering $\delta_{[n]} = \epsilon\delta_1 + \epsilon^3\delta_3 + ... + \epsilon^{2n+1}\delta_{2n+1}$ could be adopted for the hyperstatic unknown without loss of generality).

Once all the hyperstatic coefficients $\delta_i$ have been assessed, the unique compatible function $z_{[n]}$ is determined by substituting the solutions (24)-(26) into the functions (17). Therefore, by inverting the change of coordinates, the static configuration of the cable is asymptotically expressed by the configurational function $y_{[n]}(x) = y_0(x) + \epsilon y_1(x) + \epsilon^2 y_2(x) + ... + \epsilon^i y_i(x) + ... + \epsilon^n y_n(x)$, where the series terms are

$$\epsilon^i : \qquad y_i(x) = \sum_{j=0}^{i+1} d_{ij}x^j = d_{i1}x + d_{i2}x^2 + ... + d_{i(i+1)}x^{i+1} \tag{27}$$

where the parameter-dependent coefficients $d_{ij}$ are reported in the Appendix A (for $i = 1, ..., 6$).

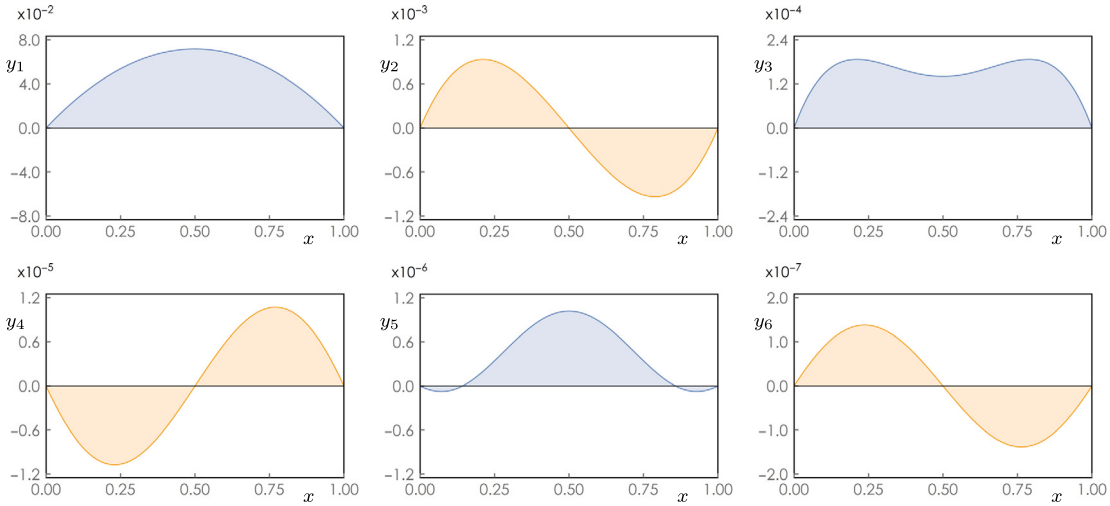


**Fig. 2.** Perturbation solutions $y_i(x)$ of increasing orders $(i = 1, .., 6)$ for the inclined shallow cable with aspect ratio $\Lambda = 101/100$ and inclination angle $\vartheta = \pi/8$.

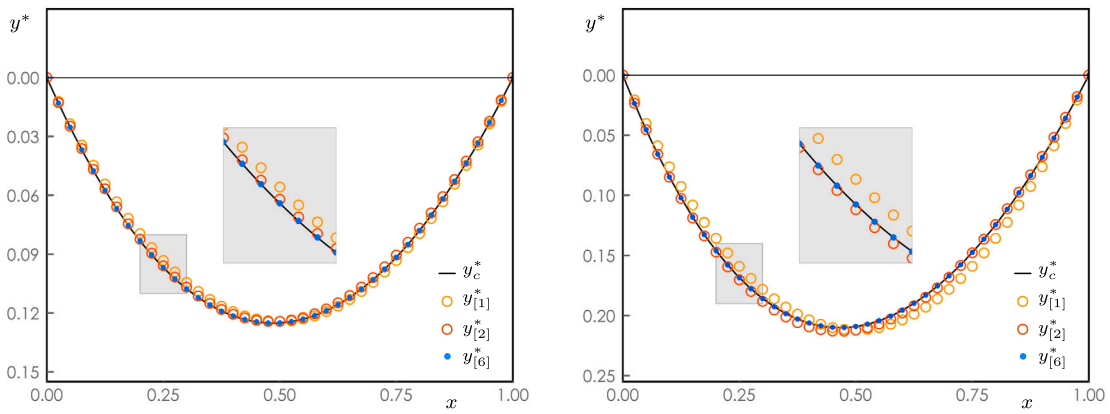


**Fig. 3.** Comparison of the catenary solution $y_c^*(x)$ and its asymptotic approximations $y_{[n]}^*(x)$ of orders $n = 1, 2, 6$ for the inclined shallow cable characterized by aspect ratio $\Lambda = 103/100$ and different inclination angles: (a) $\vartheta = \pi/8$, (b) $\vartheta = \pi/4$.

In synthesis, the noteworthy physical-mathematical achievement is that the configurational cable function $y_{[n]}(x)$ is determined as a known fully analytical – although asymptotically approximate – function of the mechanical parameter pair $(\Lambda, \vartheta)$. From the mechanical viewpoint, it may be important to recognize that the lowest-order configurational function $y_{[1]}(x)$ describes the well-known and widely used parabolic (symmetric) configuration, whereas the second-order configurational function $y_{[2]}(x)$ describes the less-known cubic (non-symmetric) configuration (described for instance in Example 2.1 of the Irvine monograph [1]). As general result, odd $(i = 1, 3, 5, ...)$ and even $(i = 2, 4, 6, ...)$ terms $y_i(x)$ describe symmetric and anti-symmetric contributions (over the $x$-domain) to the cable configurations, respectively. All the anti-symmetric terms vanish for leveled supports, as expected. The full set $(i = 1, ..., 6)$ of functions $y_i(x)$ is illustrated in Fig. 2 for a particular inclined shallow cable (the zero-th order linear function $y_0(x) = x \tan \vartheta$ is not reported). Qualitatively, the symmetry (blue curves) and anti-symmetry (red curves) of the even-order and odd-order functions can be recognized. As a minor remark, anti-symmetric odd terms do not contribute to the midspan sag. Quantitatively, the growing smallness of the function amplitudes for increasing orders can be verified.

Parametric analyses comparing the exact catenary function $y_c(x)$ and its asymptotic approximations $y_{[n]}(x)$ for different combinations the mechanical parameters $(\vartheta, \Lambda)$ are illustrated in Fig. 3. The auxiliary differences $y_c^*(x) = y_c(x) - y_0(x)$ and $y_{[n]}^*(x) = y_{[n]}(x) - y_0(x)$ can be defined to exalt the comparison by filtering out the dominant (zero-th order) effect of the chord inclination. The comparison shows how the lowest order approximation $y_{[1]}^*(x)$ (orange circles) and $y_{[2]}^*(x)$ (red circles) suffice to match the exact catenary $y_c^*(x)$ (black curve) with good accuracy. The cubic function $y_{[2]}^*(x)$ satisfyingly captures the appreciable loss of symmetry that characterizes in particular the cable with higher inclination (Fig. 3b). Excellent agreement is reached by the highest-order approximation function $y_{[6]}^*(x)$ (blue dots), independently of the inclination angle. The accuracy of the asymptotic approximations is also verified quantitatively by the results (and relative errors) reported for the midspan sag in Table 1 for a selected combination of parameters $(\Lambda, \vartheta)$. Specifically, the relative error $e_n^y = [y_{[n]}(1/4) - y(1/4)]/y(1/4)$ decreases up to $2 \times 10^{-7}$ for $n = 6$. As last remark, the $\Lambda$-values selected in the parametric analyses correspond to sag-to-span ratios falling in the range $1/10$ to $1/5$

**Table 1**
Asymptotically approximate configurational function $y_{[n]}(x)$, horizontal reaction $h_{[n]}$ and vertical reaction $v_{[n]}$ for the inclined shallow cable characterized by aspect ratio $\Lambda = 101/100$ and inclination angle $\vartheta = \pi/8$. Comparison with the exact catenary values and relative errors for increasing approximation orders $n$.

| | $y_{[n]}(1/4)$ | $e_n^y$ | $h_{[n]}$ | $e_n^h$ | $v_{[n]}$ | $e_n^v$ |
|---|---|---|---|---|---|---|
| $n=1$ | 0.05380792 | 0.0197438 | 3.484617 | 0.0078069 | 1.443376 | -0.4145596 |
| $n=2$ | 0.05471782 | -0.0031675 | 3.484617 | 0.0078069 | 2.443376 | -0.0089545 |
| $n=3$ | 0.05490186 | 0.0001853 | 3.457389 | -0.0000678 | 2.465918 | 0.0001887 |
| $n=4$ | 0.05489122 | -0.0000085 | 3.457389 | -0.0000678 | 2.465918 | 0.0001887 |
| $n=5$ | 0.05489157 | -0.0000023 | 3.457626 | 0.0000006 | 2.465445 | -0.0000030 |
| $n=6$ | 0.05489170 | 0.0000002 | 3.457626 | 0.0000006 | 2.465445 | -0.0000030 |
| Catenary | 0.05489169 | - | 3.457624 | - | 2.465453 | - |

(see Fig. 3), that largely covers the typical shallowness of structural cables (whose sag-to-span ratios generally do not exceed $1/10$ or $1/8$). Naturally, the accuracy of the asymptotic approximation is expected to degrade for non-shallow cables. However, errors $e_n^y < 2\times10^{-3}$ are still achievable by the highest-order approximation ($n=6$) for very large sag-to-span ratios (say $1/3$ or more).

From the algorithmic viewpoint, it is convenient to define the derivative $\psi(x) = y'(x)$, whose asymptotic expression is $\psi_{[n]} = \psi_0(x)+\epsilon\psi_1(x)+\epsilon^2\psi_2(x)+...+\epsilon^i\psi_i(x)+...+\epsilon^n\psi_n(x)$, where the series coefficient functions are $\psi_i(x) = \sum_{j=0}^{i+1} j\, d_{ij} x^{(j-1)}$. Furthermore, it is convenient to introduce the quantity $\varphi = \psi(0) = \tan\theta$, corresponding to the value attained by the function $\psi(x)$ at the left support, whose asymptotic expression is $\varphi_{[n]} = \varphi_0 + \epsilon\varphi_1 + \epsilon^2\varphi_2 + ... + \epsilon^i\varphi_i + ... + \epsilon^n\varphi_n$, where the series coefficients are $\varphi_i = \psi_i(0) = d_{i1}$.

Once the hyperstatic unknown $\delta$ and the configurational function $y(x)$ have been (asymptotically) determined, the horizontal reaction $h$ and vertical reaction $v$, together with the $x$-dependent axial force $n(x)$ can be determined according to the (exact) relations

$$h = \frac{\cos\vartheta}{4\Lambda\delta}, \qquad v = h\varphi = \frac{\cos\vartheta}{4\Lambda\delta}\varphi, \qquad n(x) = h\left[1+(\psi(x))^2\right]^{1/2} = \frac{\cos\vartheta}{4\Lambda\delta}\left[1+(\psi(x))^2\right]^{1/2} \tag{28}$$

which can be employed to achieve the corresponding asymptotic expressions, by consistently employing the series expansion of the variables $\delta$, $\varphi$, $\psi(x)$ and the ordering of the parameter $\Lambda$.

Starting with the horizontal reaction, the asymptotic expression can be determined in the series form $h_{[n]} = \epsilon^{-1}h_1 + \epsilon^0 h_2 + \epsilon^1 h_3 + \epsilon^2 h_4 + ... + \epsilon^{i-2}h_i + ... + \epsilon^{n-2}h_n$. It is particularly important to note that – consistently with the perturbation scheme – the $i$-th term of the series belongs to the $(i-2)$-th order $\mathcal{O}(\epsilon^{i-2})$ and, consequently, the lowest-order approximation $h_{[1]} \in \mathcal{O}(\epsilon^{-1})$. Methodologically, this finding is a necessary consequence of the assumption of cable shallowness (10), and cannot be introduced as independent hypothesis. Physically, this mathematical result formalizes the mechanical concept that shallow cables have large horizontal reactions, which – as literally first approximation – are inversely proportional to the small midspan sag. Recalling the consistency condition $\Lambda = 1+\epsilon^2\Lambda_2$ and the asymptotic expression $\delta_{[n]}$, after new series expansion and collection of the same $\epsilon$-power terms, the odd coefficients of the series read

$$h_1 = \frac{\cos\vartheta}{4\delta_1} \tag{29}$$

$$h_3 = -\left[\frac{\Lambda_2}{4\delta_1} + \frac{\delta_3}{4\delta_1^2}\right]\cos\vartheta \tag{30}$$

$$h_5 = \left[\frac{\Lambda_2^2}{4\delta_1} + \frac{\Lambda_2\delta_3-\delta_5}{4\delta_1^2} + \frac{\delta_3^2}{4\delta_1^3}\right]\cos\vartheta \tag{31}$$

while even coefficients $h_2$, $h_4$, ... are systematically null. Interestingly, coefficient $h_3$ becomes null for the particular inclination angle $\vartheta_c = \arccos(2\sqrt{2}/5) \simeq 1$. The physical consequence of this remark is that the lowest-order approximations $h_{[1]}$ systematically overestimates or underestimates the exact horizontal reaction for low ($\vartheta < \vartheta_c$) and high ($\vartheta > \vartheta_c$) inclination angles, respectively.

Next, the asymptotic expression of the vertical reaction can be determined in the series form $v_{[n]} = \epsilon^{-1}v_1 + \epsilon^0 v_2 + \epsilon^1 v_3 + \epsilon^2 v_4 + ... + \epsilon^{i-2}v_i + ... + \epsilon^{n-2}v_n$. Similarly to the horizontal reaction, the $i$-th term of the series belongs to the $(i-2)$-th order $\mathcal{O}(\epsilon^{i-2})$ and, consequently, the lowest-order approximation $v_{[1]} \in \mathcal{O}(\epsilon^{-1})$ for inclined cables. By recalling the consistent ordering of the parameter $\Lambda$ and the asymptotic expressions $\delta_{[n]}$ and $\varphi_{[n]}$ and after some algebra, the odd coefficients of the series read

$$v_1 = \frac{\varphi_0}{4\delta_1}\cos\vartheta \tag{32}$$

$$v_3 = \left[-\frac{\Lambda_2\varphi_0}{4\delta_1} - \frac{\delta_3\varphi_0}{4\delta_1^2} + \frac{\varphi_2}{4\delta_1}\right]\cos\vartheta \tag{33}$$

$$v_5 = \left[\frac{\Lambda_2^2\varphi_0}{4\delta_1} + \frac{\Lambda_2\delta_3\varphi_0}{4\delta_1^2} - \frac{\Lambda_2\varphi_2}{4\delta_1} + \frac{\delta_3^2\varphi_0}{4\delta_1^3} + \frac{\varphi_4}{4\delta_1} - \frac{\delta_5\varphi_0}{4\delta_1^2} - \frac{\delta_3\varphi_2}{4\delta_1^2}\right]\cos\vartheta \tag{34}$$

while the even coefficients of the series, whose expressions are not reported for the sake of synthesis, can be demonstrated (after substitutions and some mathematical manipulations) to be either unitary $v_2 = 1$ (lowest even order), or null $v_4 = v_6 = ... = 0$ (all

higher even orders). Moreover, by recalling that $\varphi_0 = \tan\vartheta$, it can be found that $\nu_1 = 0$ for inclination angle $\vartheta = 0$. Physically, this mathematical result states that the first-order term $\nu_1$ aligns the support reaction $r_1 = (h_1^2 + v_1^2)^{1/2}$ along the chord direction (and is null for not inclined cables), while the second-order term $\nu_2$ accounts for half the total self-weight of the cable.

Finally, the asymptotic expression of the axial force can be determined in the series form $n_{[n]}(x) = \epsilon^{-1} n_1(x) + \epsilon^0 n_2(x) + \epsilon^1 n_3(x) + \epsilon^2 n_4(x) + \ldots + \epsilon^{i-2} n_i(x) + \ldots + \epsilon^{n-2} n_n(x)$. By recalling the consistent ordering of the parameter $\Lambda$ and the asymptotic expressions $\delta_{[n]}$ and $\psi_{[n]}(x)$, the series coefficients read

$$n_1(x) = h_1 \sec\vartheta \tag{35}$$

$$n_2(x) = h_1 \psi_1(x) \sin\vartheta \tag{36}$$

$$n_3(x) = h_3 \sec\vartheta + h_1 \psi_2 \sin\vartheta + \tfrac{1}{2} h_1 (\psi_1(x))^2 \cos^3\vartheta \tag{37}$$

$$n_4(x) = \left[h_3 \psi_1(x) + h_1 \psi_3(x)\right] \sin\vartheta + h_1 \psi_1(x) \psi_2(x) \cos^3\vartheta - \tfrac{1}{2} h_1 (\psi_1(x))^3 \sin\vartheta \cos^4\vartheta \tag{38}$$

$$\begin{aligned} n_5(x) = {} & h_5 \sec\vartheta + \left[h_3 \psi_2(x) + h_1 \psi_4(x)\right] \sin\vartheta + \\ & + \left[\tfrac{1}{2} h_3 (\psi_1(x))^2 + h_1 \left(\tfrac{1}{2} (\psi_2(x))^2 + \psi_1(x) \psi_3(x)\right)\right] \cos^3\vartheta + \\ & + \tfrac{1}{16} h_1 (\psi_1(x))^4 (8 - 5\cos^2\vartheta) \cos^5\vartheta - \tfrac{3}{2} h_1 (\psi_1(x))^2 \psi_2(x) \sin\vartheta \cos^4\vartheta \end{aligned} \tag{39}$$

$$\begin{aligned} n_6(x) = {} & \left[h_5 \psi_1(x) + h_3 \psi_3(x) + h_1 \psi_5(x)\right] \sin\vartheta + \\ & + \left[h_3 \psi_1(x) \psi_2(x) + h_1 \left(\psi_2(x) \psi_3(x) + \psi_1(x) \psi_4(x)\right)\right] \cos^3\vartheta + \\ & + \tfrac{1}{4} h_1 (\psi_1(x))^3 \psi_2(x) (8 - 5\cos^2\vartheta) \cos^5\vartheta + \tfrac{1}{32} h_1 (\psi_1(x))^5 (7\sin(3\vartheta) - 9\sin\vartheta) \cos^6\vartheta + \\ & - \tfrac{1}{2} \left[h_3 (\psi_1(x))^3 + 3 h_1 \psi_1(x) (\psi_2(x))^2 + 3 h_1 (\psi_1(x))^2 \psi_3(x)\right] \sin\vartheta \cos^4\vartheta \end{aligned} \tag{40}$$

where it can be noted that the lowest term is actually $x$-independent, and also $n_1(x) = h_1$ for inclination angle $\vartheta = 0$. Physically, this mathematical result consistently supports the diffused simplifying assumption consisting in approximating the $x$-dependent axial tension with the dominant part of its constant component aligned along the chord direction.

Parametric analyses comparing the exact horizontal reactions $h$ and its asymptotic approximations $h_{[n]}$ over the technically relevant range of the mechanical parameters $(\vartheta, \Lambda)$ are illustrated in Fig. 4 for low ($n = 2$) and high ($n = 6$) approximation orders. The comparison shows that the lowest order approximations $h_{[2]}$ (yellow surface in Fig. 4a) already matches the exact horizontal reaction $h$ (black dots) with satisfying accuracy. Specifically, the relative error $e_n^h = (h_{[n]} - h)/h$ for the horizontal reaction is sufficiently low for many applications (namely $|e_2^h| < 3 \times 10^{-2}$, see Fig. 4b). Good and excellent agreement are achieved by the higher order approximations $h_{[4]}$ (here not reported for the sake of synthesis) and $h_{[6]}$ (green surface in Fig. 4c), respectively, with very low and extremely low errors (namely $|e_4^h| < 8 \times 10^{-4}$ and $|e_6^h| < 3 \times 10^{-5}$, see Fig. 4d). Qualitatively similar considerations can be pointed out for the comparison of the exact vertical reactions $v$ and its asymptotic approximations $\nu_{[n]}$ (Fig. 5). From the quantitative viewpoint, the vertical reactions $v$ shows slightly higher values of the relative error $e_n^v = (\nu_{[n]} - \nu)/\nu$ (namely $|e_2^v| < 6 \times 10^{-2}$, $|e_4^v| < 5 \times 10^{-3}$ and $|e_6^v| < 4 \times 10^{-4}$, see Fig. 5b,d), that can be related to the asymptotic approximation of the variable $\varphi$ (see equations (28)). The quantitative accuracy of the asymptotic approximations is also verified by the results reported in Table 1 for a selected $(\Lambda, \vartheta)$-combination.

## 3. Geometric stiffness matrix

The *catenary stiffness matrix* can formally be defined as the square matrix governing the linearized algebraic vector relationship between the boundary forces and the boundary displacements that can be imposed at the supports of the catenary cable. Specifically, the catenary stiffness matrix has fully geometric (non elastic) nature, due to the cable inextensibility. Indeed, within the framework of the direct stiffness method, the inextensible catenary cable can be regarded as a pretensioned member, connecting displaceable supports (nodes). By assuming known the pretension, the boundary forces must be properly defined as the *incremental* (linearized) nodal forces associated to *small* boundary displacements, intended as (infinitesimal) nodal displacements that slightly modify the static equilibrium configuration associated to fixed supports.

Coherently with the computational algorithms of the direct stiffness method for multi-member structures, it may be convenient to express all the nodal variables (forces and displacements) in a global right-handed cartesian reference systems (Fig. 1). Accordingly, the nodal force vectors $\boldsymbol{F}_A = (F_A^H, F_A^V)$ and $\boldsymbol{F}_B = (F_B^H, F_B^V)$, and the nodal displacement vectors $\boldsymbol{S}_A = (S_A^X, S_A^Y)$ and $\boldsymbol{S}_B = (S_B^X, S_B^Y)$ can be defined, by using the subscripts to distinguish the supports $\mathcal{S}_A$ and $\mathcal{S}_B$. Therefore, the nondimensional vectors $\boldsymbol{f}_A = (f_A^h, f_A^v)$, $\boldsymbol{f}_B = (f_B^h, f_B^v)$, $\boldsymbol{s}_A = (s_A^x, s_A^y)$, $\boldsymbol{s}_B = (s_B^x, s_B^y)$ can also be defined, by introducing the dimensionless variables

$$f_A^h = \frac{2F_A^H}{wL_0}, \qquad f_A^v = \frac{2F_A^V}{wL_0}, \qquad f_B^h = \frac{2F_B^H}{wL_0}, \qquad f_B^v = \frac{2F_B^V}{wL_0}, \qquad s_A^x = \frac{S_A^X}{L}, \qquad s_A^y = \frac{S_A^Y}{L}, \qquad s_B^x = \frac{S_B^X}{L}, \qquad s_B^y = \frac{S_B^Y}{L} \tag{41}$$

which can be collected in the four-by-one column vectors $\boldsymbol{f} = (f_A^h, f_A^v, f_B^h, f_B^v)^\top$ and $\boldsymbol{s} = (s_A^x, s_A^y, s_B^x, s_B^y)^\top$.

On the base of static considerations, the four components of the nodal forces can straightforwardly be associated to the two components of the nondimensional vector of boundary reactions $\boldsymbol{r} = (h, v)$ by the relations $f_A^h = -h$, $f_A^v = v$, $f_B^h = h$, $f_B^v = 2 - v$.

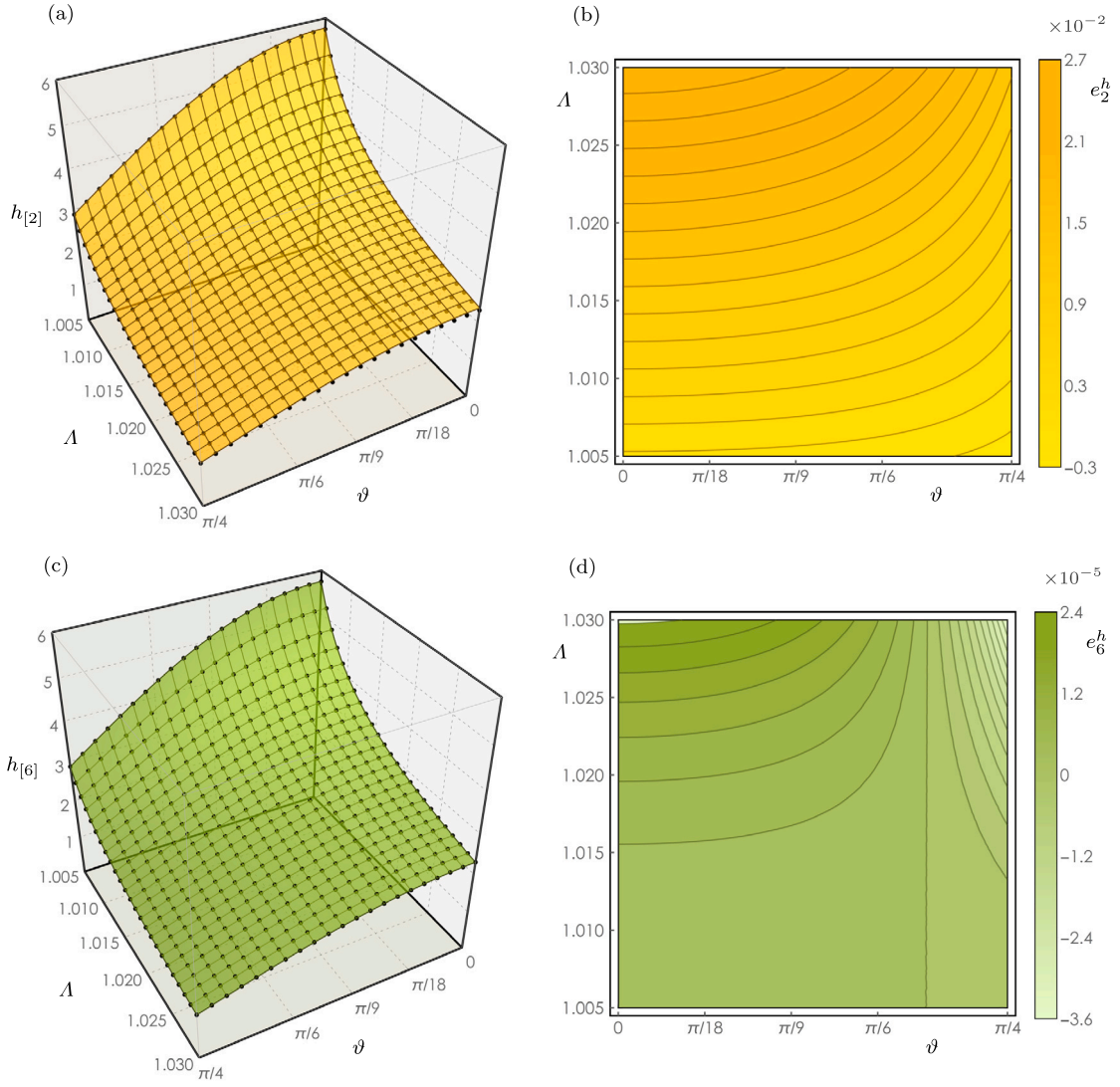


**Fig. 4.** Exact horizontal reaction $h$ (black dots) versus asymptotic approximations $h_{[n]}$ for varying mechanical parameters in the relevant range of aspect ratios $\Lambda \in [1005/1000, 1030/1000]$ and inclination angles $\vartheta \in [0, \pi/4]$: (a),(b) $h_{[2]}$ (yellow surface) and $e_2^h$ (yellow contour plot), (c),(d) $h_{[6]}$ (green surface) and $e_6^h$ (green contour plot).

Similarly, on the base of geometric considerations, the four components of the nodal displacements can immediately be associated to the four components of the nondimensional column vector of boundary displacements $\boldsymbol{x} = (x_A, y_A, x_B, y_B)^\top$ by the relations $s_A^x = x_A$, $s_A^y = -y_A$, $s_B^x = x_B$, $s_B^y = -y_B$ (Fig. 1). Consequently, the nodal force differential $d\boldsymbol{f}$ and the nodal displacement differential $d\boldsymbol{s}$ relate with the differentials of the boundary reaction $d\boldsymbol{r}$ and boundary displacements $d\boldsymbol{x}_A$ and $d\boldsymbol{x}_B$ according to the linear matrix relations

$$d\boldsymbol{f} = \mathbf{R}\, d\boldsymbol{r}, \qquad d\boldsymbol{s} = \mathbf{S}\, d\boldsymbol{x} \tag{42}$$

where $\mathbf{R}$ and $\mathbf{S}$ are proper four-by-two and four-by-four matrices, respectively, that can be expressed as $\mathbf{R} = \left(\mathbf{I}_1, \mathbf{I}_2\right)^\top$ and $\mathbf{S} = \operatorname{diag}\left(\mathbf{I}_2, \mathbf{I}_2\right)$, with $\mathbf{I}_1 = \operatorname{diag}(-1, 1)$ and with $\mathbf{I}_2 = \operatorname{diag}(1, -1)$.

Physically, the differentials in equation (42) express the incremental nodal forces $d\boldsymbol{f}$ determined by small nodal displacements $d\boldsymbol{s}$, geometrically relatable to the small support displacements $d\boldsymbol{x}$ that cause a slight increment $d\boldsymbol{r}$ in the catenary cable reactions. Consequently, assessing the geometric stiffness matrix of the catenary cable reduces to determine the linear relation between the incremental reactions $d\boldsymbol{r}$ and the small nodal displacements $d\boldsymbol{x}$. Formally, the relation is expressed for each reaction component in the vector form

$$dh = \mathbf{k}_h\, d\boldsymbol{x}, \qquad dv = \mathbf{k}_v\, d\boldsymbol{x} \tag{43}$$

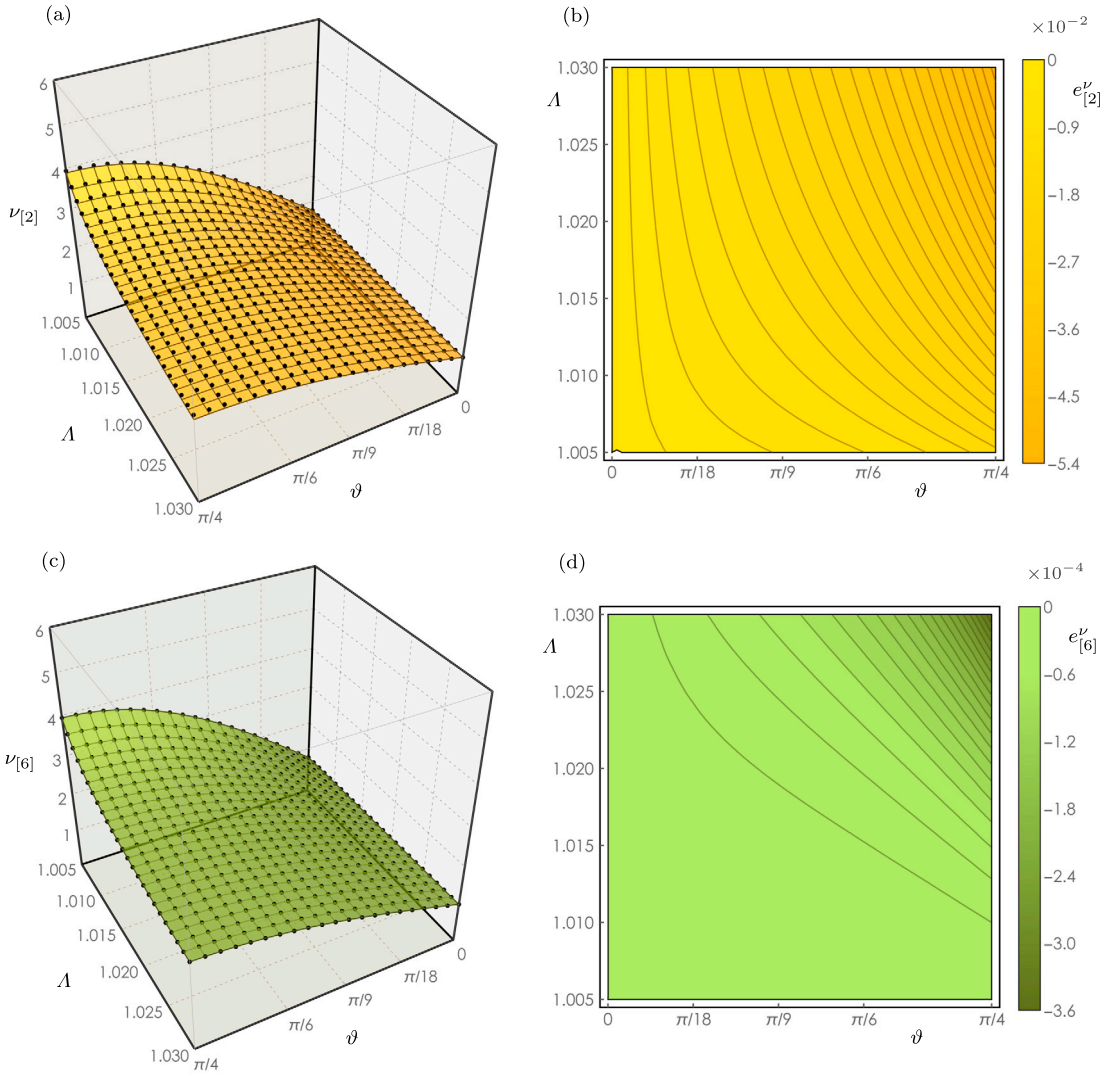


**Fig. 5.** Exact vertical reaction $\nu$ (black dots) versus asymptotic approximations $\nu_{[n]}$ for varying mechanical parameters in the relevant range of aspect ratios $\Lambda \in [1005/1000, 1030/1000]$ and inclination angles $\vartheta \in [0, \pi/4]$: (a),(b) $\nu_{[2]}$ (blue surface) and $e^{\nu}_{[2]}$, (c),(d) $\nu_{[4]}$ (yellow surface) and $e^{\nu}_{[4]}$, (e),(f) $\nu_{[6]}$ (green surface) and $e^{\nu}_{[6]}$.

where $\mathbf{k}_h$ and $\mathbf{k}_v$ are one-by-four row matrices (*stiffness row matrices*), whose elements can be regarded as (first) sensitivities of the horizontal reaction $\boldsymbol{r}$ with respect to the boundary displacements $\boldsymbol{x}$, but also as (unknown) stiffness coefficients. Therefore, by employing equations (42), the incremental nodal forces $d\boldsymbol{f}$ are finally related to the small nodal displacements $d\boldsymbol{s}$ by the linear relation

$$d\boldsymbol{f} = \mathbf{R}\, d\boldsymbol{r} = \mathbf{R} \begin{pmatrix} \mathbf{k}_h \\ \mathbf{k}_v \end{pmatrix} d\boldsymbol{x} = \mathbf{R} \begin{pmatrix} \mathbf{k}_h \\ \mathbf{k}_v \end{pmatrix} \mathbf{S}\, d\boldsymbol{s} = \mathbf{K}\, d\boldsymbol{s} \tag{44}$$

where $\mathbf{K}$ is the sought-for four-by-four stiffness matrix of the catenary inextensible cable. For its definition, the fundamental issue is the analytical assessment of the vector stiffness row matrices $\mathbf{k}_h$ and $\mathbf{k}_v$.

### 3.1. Catenary stiffness matrix

Determining the stiffness coefficients $\mathbf{k}_h$ and $\mathbf{k}_v$ governing the analytical relation between support reactions and boundary displacements requires to update the exact solution of the nonlinear differential equation (3) by taking into account the general boundary conditions $y(x_A) = y_A$ and $y(1 + x_B) = \tan\vartheta + y_B$. By recalling the properties of hyperbolic functions, the statically determinable solutions have the analytical form

$$y_k(x) = y_A + \frac{\sinh\big(4\delta_k(x - x_A)\big)\sinh\big(\Psi_k - 4\delta_k(x + x_A)\big)}{4\delta_k} \tag{45}$$

where the nondimensional auxiliary quantity $\Psi_k$ depends on all the boundary displacements

$$\Psi_k = 4\delta_k(1 + x_A + x_B) + \operatorname{arcsinh}\left[\frac{4\delta_k\,(\tan\vartheta - y_A + y_B)}{\sinh\left(4\delta_k\,(1 - x_A + x_B)\right)}\right] \tag{46}$$

while $\delta_k$ plays again the role of hyperstatic unknown to be assessed a posteriori, and the subscript $k$ indicates that it depends on the boundary displacements $\boldsymbol{x}$ and generally differs from the $\boldsymbol{x}$-independent unknown $\delta$.

The compatibility equation required for the univocal assessment of the hyperstatic unknown $\delta_k$ that identifies the unique geometrically compatible solution, among all the statically determinable functions $y_k(x)$, is provided by the inextensibility condition $\Lambda_k = \Lambda$, where the arc-length has the analytical form

$$\Lambda_k = \cos\vartheta \int_{x_A}^{1+x_B} \left[1 + \left(y_k'\right)^2\right]^{\frac{1}{2}} \mathrm{d}x = \frac{\cos\vartheta}{4\delta_k} \sinh\left(4\delta_k(1 - x_A + x_B)\right) \cosh\left(\Psi_k - 4\delta_k(1 + x_A + x_B)\right) \tag{47}$$

which can be proved to depend on the displacement differences $\Delta_x = x_B - x_A$ and $\Delta_y = y_B - y_A$ only. Naturally, the solution $y_k(x)$ can be easily demonstrated to recover the catenary solution $y_c(x)$, for vanishing boundary displacements or, more generally, for null differences $\Delta_x = 0$ and $\Delta_y = 0$.

Although not necessary for determining the geometric stiffness matrix, the catenary configuration can be obtained by slightly updating the solution strategy already outlined for fixed supports. Briefly, the inextensibility condition establishes the compatibility equation $\Lambda_k = \Lambda$. The assigned aspect ratio $\Lambda$ must satisfy the updated admissibility inequality $\Lambda > \Lambda_d$, where the quantity $\Lambda_d = \cos\vartheta\,[(1 + \Delta_x)^2 + (\tan\vartheta + \Delta_y)^2]^{1/2}$ is the distance between the displaced supports. Being strongly nonlinear, the compatibility equation has not an explicit analytical solution and has to be solved numerically to assess the compatible hyperstatic unknown $\delta_k$. Once the hyperstatic unknown $\delta_k$ has been assessed, the configurational function $y_k(x)$ is determined, while the horizontal and vertical reactions can be calculated according to the formulas $h = \cos\vartheta/(4\Lambda\delta_k)$ and $v = \cos\vartheta/(4\Lambda\delta_k)\sinh(\Psi_k - 8\delta_k\,x_A)$. Further details can be found in a dedicated technical note [34].

Focusing instead on the catenary stiffness matrix, the leading idea is that – even if the support reactions $\boldsymbol{r}$ cannot be explicitly related to the boundary displacements $\boldsymbol{x}$ – their differential $d\boldsymbol{r}$ can instead be expressed analytically, as parametric functions of the differential of the boundary displacement $d\boldsymbol{x}$. To this end, it is convenient to express the compatibility equation in the form

$$\mathfrak{F}_k(h, \boldsymbol{x}) = \Lambda_k(h, \boldsymbol{x}) - \Lambda = 0 \tag{48}$$

where the formula $\delta_k = \cos\vartheta/(4\Lambda h)$ can be employed in equation (47) to adopt the reaction $h$ as primary unknown in the arc length $\Lambda_k(h, \boldsymbol{x})$. Although the implicit function $\mathfrak{F}_k(h, \boldsymbol{x}) = 0$ does not admit explicit form $h = \mathfrak{f}_k(\boldsymbol{x})$, its total differential in the space of boundary displacements can be formally defined as $dh = \nabla\mathfrak{f}_k \cdot d\boldsymbol{x}$. Consequently, the stiffness row matrix $\mathbf{k}_h$ defined in equations (43) mathematically corresponds to the transpose of the gradient column vector $\nabla\mathfrak{f}_k$, evaluated at $\boldsymbol{x} = \mathbf{0}$. Specifically, by introducing the component form of the operator $\nabla = (\partial/\partial x_A, \partial/\partial y_A, \partial/\partial x_B, \partial/\partial y_B)$, the row matrix reads

$$\mathbf{k}_h = (k^h_{xA}, k^h_{yA}, k^h_{xB}, k^h_{yB}) = \left(\frac{\partial\mathfrak{f}_k}{\partial x_A}, \frac{\partial\mathfrak{f}_k}{\partial y_A}, \frac{\partial\mathfrak{f}_k}{\partial x_B}, \frac{\partial\mathfrak{f}_k}{\partial y_B}\right)_{\boldsymbol{x}=\mathbf{0}} \tag{49}$$

where, recalling that $\mathfrak{F}_k(h, \boldsymbol{x})$ depends on the displacement differences only, the four matrix coefficients can be demonstrated to have the relevant symmetry properties $k^h_{xB} = -k^h_{xA} =: k^h_x$ and $k^h_{yB} = -k^h_{yA} =: k^h_y$. Therefore, the partial derivatives in equation (49) can be determined analytically by invoking the Implicit Function Theorem for the differentiable function $\mathfrak{F}_k(h, \boldsymbol{x})$, yielding

$$k^h_x = \left[-\frac{\partial\mathfrak{F}_k}{\partial x_B}\left(\frac{\partial\mathfrak{F}_k}{\partial h}\right)^{-1}\right]_{\boldsymbol{x}=\mathbf{0}} = \frac{\cos\vartheta}{\Lambda\left[4\delta - \tanh(4\delta)\right]} \tag{50}$$

$$k^h_y = \left[-\frac{\partial\mathfrak{F}_k}{\partial y_B}\left(\frac{\partial\mathfrak{F}_k}{\partial h}\right)^{-1}\right]_{\boldsymbol{x}=\mathbf{0}} = \frac{8\delta\sin\vartheta\,\operatorname{csch}(8\delta)}{\Lambda\left[4\delta - \tanh(4\delta)\right]} \tag{51}$$

where the identity $\left[\delta_k\right]_{\boldsymbol{x}=\mathbf{0}} = \delta$ has been employed. It may be worth noting that the Theorem requires that the derivative $\partial\mathfrak{F}_k/\partial h$ differs from zero at $\boldsymbol{x} = \mathbf{0}$, which is a physically acceptable assumption.

Similarly to the horizontal reaction, the vertical reaction cannot be expressed as an explicit analytical function of the boundary displacements. Nonetheless, the relation $v = \mathfrak{g}_k(h, \boldsymbol{x}) = h\sinh(\Psi_k - 8\delta\,x_A)$ holds (updated *hyperstatic relation*). Therefore, by recalling that $h = \mathfrak{f}_k(\boldsymbol{x})$, the total differential of the composite function $v = \mathfrak{g}_k(\mathfrak{f}_k(\boldsymbol{x}), \boldsymbol{x})$ can be determined as $dv = (\nabla\mathfrak{g}_k + \mathfrak{g}_k'\nabla\mathfrak{f}_k) \cdot d\boldsymbol{x}$ (where the apex indicates derivative with respect to the variable $h$). Accordingly, the stiffness row matrix $\mathbf{k}_v$ mathematically represents the transpose of the column vector $\nabla\mathfrak{g}_k + \mathfrak{g}_k'\nabla\mathfrak{f}_k$, evaluated at $\boldsymbol{x} = \mathbf{0}$. In component form, the matrix reads

$$\mathbf{k}_v = (k^v_{xA}, k^v_{yA}, k^v_{xB}, k^v_{yB}) = \left(\frac{\partial\mathfrak{g}_k}{\partial x_A} + \mathfrak{g}_k'\frac{\partial\mathfrak{f}_k}{\partial x_A}, \frac{\partial\mathfrak{g}_k}{\partial y_A} + \mathfrak{g}_k'\frac{\partial\mathfrak{f}_k}{\partial y_A}, \frac{\partial\mathfrak{g}_k}{\partial x_B} + \mathfrak{g}_k'\frac{\partial\mathfrak{f}_k}{\partial x_B}, \frac{\partial\mathfrak{g}_k}{\partial y_B} + \mathfrak{g}_k'\frac{\partial\mathfrak{f}_k}{\partial y_B}\right)_{\boldsymbol{x}=\mathbf{0}} \tag{52}$$

where the row coefficients can be demonstrated to have the relevant symmetry properties $k^v_{xB} = -k^v_{xA} =: k^v_x$ and $k^v_{yB} = -k^v_{yA} =: k^v_y$.

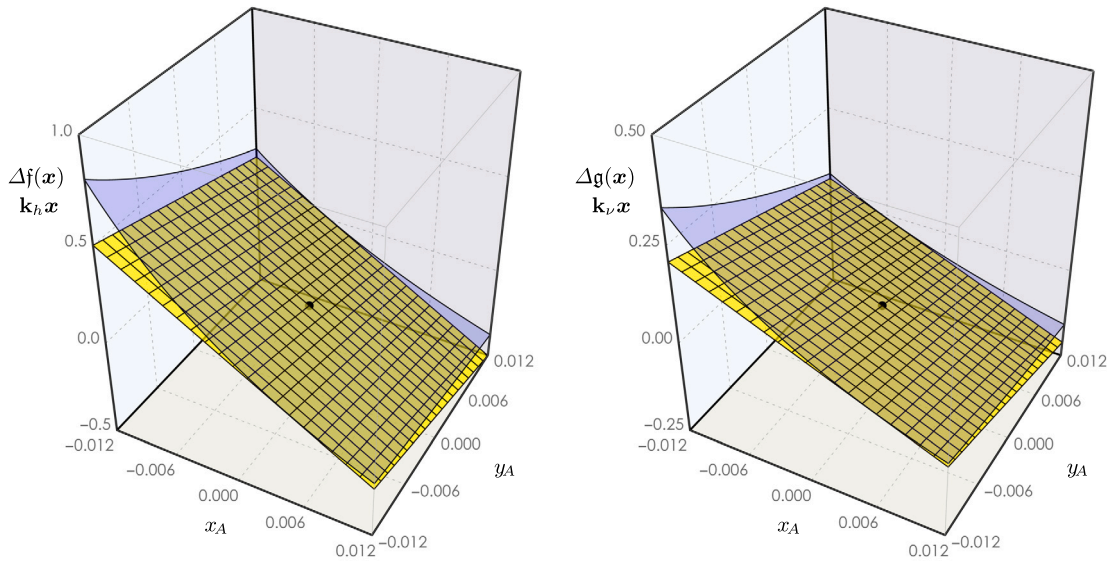


**Fig. 6.** Numerical comparison of the horizontal and vertical reactions determined according to the stiffness matrix $\mathbf{k}_h\boldsymbol{x}$ and $\mathbf{k}_v\boldsymbol{x}$ (yellow planes) and the exact expressions $\Delta\mathfrak{f}(\boldsymbol{x})$ and $\Delta\mathfrak{g}(\boldsymbol{x})$ (light blue surfaces) over an admissible range of boundary displacements $\boldsymbol{x}=(x_A,y_A,0,0)$ for fixed values of the aspect ratio $\Lambda=103/100$ and inclination angle $\vartheta=\pi/8$.

The partial derivatives can be determined analytically, yielding

$$k_x^v=\left[\frac{\partial\mathfrak{g}_k}{\partial x_B}-\mathfrak{g}_k'\frac{\partial\mathfrak{F}_k}{\partial x_B}\left(\frac{\partial\mathfrak{F}_k}{\partial h}\right)^{-1}\right]_{\boldsymbol{x}=\mathbf{0}}=\frac{4\delta\sin\vartheta\,\mathrm{csch}^2(4\delta)}{\Lambda\left[4\delta-\tanh(4\delta)\right]} \tag{53}$$

$$k_y^v=\left[\frac{\partial\mathfrak{g}_k}{\partial y_B}-\mathfrak{g}_k'\frac{\partial\mathfrak{F}_k}{\partial y_B}\left(\frac{\partial\mathfrak{F}_k}{\partial h}\right)^{-1}\right]_{\boldsymbol{x}=\mathbf{0}}=\frac{\cos\vartheta\coth(4\delta)\left[4\delta-\tanh(4\delta)+256\,\delta^3\,\mathrm{csch}^2(8\delta)\tan^2\vartheta\right]}{\Lambda\left[4\delta-\tanh(4\delta)\right]} \tag{54}$$

where the relevant identity $k_x^v=k_y^h$ must be remarked. The three quantities $k_x^h$, $k_y^v$ and $k_y^h=k_x^v$ suffice to determine the catenary stiffness and will be referred as *catenary stiffness coefficients* in the following.

Once the row matrices $\mathbf{k}_h$ and $\mathbf{k}_v$ are known as functions of the mechanical parameters $(\vartheta,\Lambda)$ and the hyperstatic unknown $\delta$ of the catenary cable suspended between *fixed* supports, the geometric stiffness matrix can finally be built up according to the definition (44). After substitution, the matrix reads

$$\mathbf{K}=\begin{pmatrix} k_x^h & -k_y^h & -k_x^h & k_y^h \\ -k_x^v & k_y^v & k_x^v & -k_y^v \\ -k_x^h & k_y^h & k_x^h & -k_y^h \\ k_x^v & -k_y^v & -k_x^v & k_y^v \end{pmatrix} \tag{55}$$

where the typical form of a symmetric block matrix can be recognized. The matrix is symmetric, as can immediately be demonstrated by recalling the identity $k_x^v=k_y^h$ between the out-of-diagonal coefficients.

By considering the catenary cable suspended between fixed supports and recalling the $(\vartheta,\delta)$-dependent arc-length $\Lambda_c$ defined in equation (5), the compatibility equation provides an implicit function $\mathfrak{D}(\vartheta,\Lambda,\delta)=\Lambda_c(\vartheta,\delta)-\Lambda=0$ that does not admit explicit form $\delta=\mathfrak{d}(\vartheta,\Lambda)$. Consequently, the $\delta$-dependent catenary stiffness row matrices cannot be expressed as explicit analytical functions $\mathbf{k}_h=\mathfrak{K}_h(\vartheta,\Lambda)$ and $\mathbf{k}_v=\mathfrak{K}_v(\vartheta,\Lambda)$. Therefore, the geometric stiffness matrix $\mathbf{K}$ is a quasi-analytical function and eventually must be assessed numerically, given a certain combination of the mechanical parameters $(\vartheta,\Lambda)$. Specifically, fully numerical analyses can be carried out to verify the stiffness row matrices, by checking that the linear functions $h(\boldsymbol{x})=h+\mathbf{k}_h\boldsymbol{x}$ and $\nu(\boldsymbol{x})=\nu+\mathbf{k}_v\boldsymbol{x}$ for the horizontal and vertical reactions actually correspond to the first-order approximation of the exact nonlinear relations $\mathfrak{f}(\boldsymbol{x})$ and $\mathfrak{g}(\boldsymbol{x})$, in the proximity of the point $\boldsymbol{x}=\mathbf{0}$. Besides checking the exactness of the catenary stiffness matrix, the comparison is also useful to evaluate the validity limits of the linear approximation for the nodal force-to-displacement relationship. The comparative results over an admissible range of boundary displacements $\boldsymbol{x}$ (satisfying the inequality $(\Lambda>\Lambda_d(\boldsymbol{x}))$ are illustrated in Fig. 6 for fixed values of the aspect ratio $\Lambda$ and inclination angle $\vartheta$. The comparison highlights how the linear relations $\mathbf{k}_h\boldsymbol{x}$ and $\mathbf{k}_v\boldsymbol{x}$ correctly correspond to inclined planes (yellow) that are exactly tangent at the point $\boldsymbol{x}=\mathbf{0}$ (black dot) to the curved surfaces (light blue) corresponding to the nonlinear relations $\Delta\mathfrak{f}(\boldsymbol{x})=\mathfrak{f}(\boldsymbol{x})-h$ and $\Delta\mathfrak{g}(\boldsymbol{x})=\mathfrak{g}(\boldsymbol{x})-\nu$. From the quantitative viewpoint, the stiffness coefficients can be noted to systematically underestimate the exact support reactions.

### 3.2. Asymptotic stiffness matrix

By-passing the limits inherent to the quasi-analytical definition of the catenary stiffness matrix is crucial to achieve fully analytical and parametric solutions for complex problems related to cable structures. Specifically, an asymptotic expression of the catenary solutions for inclined cable can be a decisive advance in the formulation of mechanical problems according to the direct stiffness method. The crucial point consists in by-passing the computational bottleneck of assessing numerically (and sometimes iteratively) the hyperstatic unknowns, which do not satisfy a priori the set of compatibility equations [35–37]. Formulating the fully analytical asymptotic expression for the geometric stiffness matrix, based on the linearized relationship between nodal displacements and forces, in particular, can support the general development and solution of linear and nonlinear parametric models according to the incremental form of the direct stiffness method.

By adopting a perturbation strategy based on the key assumption of cable shallowness, methodologically similar to the approach used for inextensible cables suspended between fixed supports, the static problem accounting for displaceable supports can be reformulated by introducing an opportune change of variables

$$y(x) = y_{k0}(x) + z_k(x) = a_1 + a_0 x + z_k(x) \tag{56}$$

where the linear function $y_{k0}(x) = a_1 + a_0 x$ describes the chord between the *displaced* supports (Fig. 1). The coefficients of the function $y_{k0}(x)$ depend on the boundary displacements $\boldsymbol{x}$ according to the relations $a_0 = \Sigma_x^{-1}\left(\Delta_y + \tan\vartheta\right)$ and $a_1 = \Sigma_x^{-1}\left[y_A(1+x_B) - x_A(y_B + \tan\vartheta)\right]$, where $\Sigma_x = 1 + \Delta_x$. Applying the change of variable, the governing equation (3) becomes

$$z'' = -\delta\left[1 + a_0^2 + 2a_0 z' + \left(z'\right)^2\right]^{1/2} \tag{57}$$

while the boundary conditions read $z(0) = 0$ and $z(1) = 0$. The general equation (57) recovers the particular equation (8) for fixed supports, since $a_0 = \tan\vartheta$ and $a_1 = 0$ for vanishing boundary displacements.

Therefore, the asymptotic strategy requires to (i) postulate a series expansion in integer $\epsilon$-power series of the configurational variable $z_{k[n]}(x) = \epsilon z_{k1}(x) + \epsilon^2 z_{k2}(x) + \ldots + \epsilon^i z_{ki}(x) + \ldots + \epsilon^n z_{kn}(x)$, (ii) order the hyperstatic unknown in the form $\delta_{k[n]} = \epsilon\delta_{k1} + \epsilon^2\delta_{k2} + \ldots + \epsilon^i\delta_{ki} + \ldots + \epsilon^n\delta_{kn}$, (iii) stating and solving the linear differential system of *equilibrium perturbation equations* up to desired order, (iv) stating and solving the linear algebraic system of *compatibility perturbation equations*. As major difference with respect to the inextensible cable suspended between fixed supports, the consistency condition reads $\Lambda = \Lambda_d + \epsilon^2\Lambda_2$. By skipping all the other algorithmic details (that can be found in a dedicated technical paper [34]), the essential results are that, first, the equilibrium perturbation equations can be solved analytically and, second, the compatibility perturbation equations return fully analytical expressions for the odd hyperstatic coefficients

$$\delta_{k1} = \frac{1}{4}\frac{\Lambda_{k1}}{\cos\vartheta} \tag{58}$$

$$\delta_{k3} = -\left[\frac{3}{80} + \frac{1}{10}a_0^2\right]\frac{b_0\Lambda_{k1}\Lambda_2}{\Sigma_x\cos^2\vartheta} \tag{59}$$

$$\delta_{k5} = \left[\frac{321}{22400} + \frac{167}{1400}a_0^2 + \frac{17}{175}a_0^4\right]\frac{b_0^2\Lambda_{k1}\Lambda_2^2}{\Sigma_x^2\cos^3\vartheta} \tag{60}$$

while even coefficients $\delta_{k2}, \delta_{k4}, \ldots$ are found to be systematically null. The known zeroth-order quantities $c_0^2 = 1 + a_0^2$ and $b_0^2 = c_0^{-2}$, together with the first-order quantity $\Lambda_{k1} = (6c_0\Lambda_2\cos\vartheta)^{1/2}\Sigma_x^{-3/2}$ have been introduced. Clearly, the solutions could be extended to higher orders ($n > 6$), if necessary. Physically, it can be remarked that the hyperstatic unknown depends on the displacement differences $\Delta_x$ and $\Delta_y$ only.

Once the hyperstatic unknown $\delta_{[n]}$ and the function $z_{k[n]}(x)$ have been determined, the configurational function of the cable is asymptotically known in the consistent asymptotic form $y_{k[n]}(x) = y_{k0}(x) + z_{k[n]}(x) = y_{k0}(x) + \epsilon y_{k1}(x) + \epsilon^2 y_{k2}(x) + \ldots + \epsilon^i y_{ki}(x) + \ldots + \epsilon^n y_{kn}(x)$. Owing to the mathematical structure of the equilibrium perturbation equations, the series coefficient functions (for $i = 1, 2, \ldots$) have the polynomial expression $y_{ki}(x) = \sum_{j=1}^{i+1} a_{ij}x^j$, where $a_{ij}$ are known coefficients depending on the boundary displacements $\boldsymbol{x}$. From the algorithmic viewpoint, it is convenient to define the derivative $\psi_k(x) = y_k'(x)$, whose asymptotic expression has the form $\psi_{k[n]} = \psi_{k0}(x) + \epsilon\psi_{k1}(x) + \epsilon^2\psi_{k2}(x) + \ldots + \epsilon^i\psi_{ki}(x) + \ldots + \epsilon^n\psi_{kn}(x)$, where the series coefficient functions are $\psi_{k0}(x) = a_0$ and $\psi_{ki}(x) = \sum_{j=0}^{i+1} j\, a_{ij}x^{(j-1)}$ for $i = 1, 2, \ldots$. Furthermore, it is convenient to introduce the quantity $\varphi_k = \psi_k(x_A)$, corresponding to the value attained by the function $\psi_k(x)$ at the left *displaced* support, whose asymptotic expression has the form $\varphi_{k[n]} = \varphi_{k0} + \epsilon\varphi_{k1} + \epsilon^2\varphi_{k2} + \ldots + \epsilon^i\varphi_{ki} + \ldots + \epsilon^n\varphi_{kn}$, with $\varphi_{k0} = a_0$ and $\varphi_{ki} = \sum_{j=0}^{i+1} j\, a_{ij}x_A^{(j-1)}$ for $i = 1, 2, \ldots$. Therefore, while not a primary objective, the configurational function of the cable is determinable as fully analytical – although asymptotically approximate – function of the mechanical parameters $(\Lambda, \vartheta)$ and boundary displacements $\boldsymbol{x}$.

Focusing on the primary objective of providing an asymptotically consistent analytical expressions of the catenary stiffness matrices, the exact formulas for the horizontal and vertical reactions $h = \cos\vartheta/(4\Lambda\,\delta_k)$ and $v = \varphi_k\cos\vartheta/(4\Lambda\,\delta_k)$ can be recalled. By exploiting the known expressions $\delta_{k[n]}$ and $\varphi_{k[n]}$ and taking into account the consistency condition $\Lambda = \Lambda_d + \epsilon^2\Lambda_2$, the reactions can be asymptotically expressed in the consistent form $h_{k[n]} = \epsilon^{-1}h_{k1} + \epsilon^0 h_{k2} + \ldots + \epsilon^{i-2}h_{ki} + \ldots + \epsilon^{n-2}h_{kn}$ and $v_{k[n]} = \epsilon^{-1}v_{k1} + \epsilon^0 v_{k2} + \ldots + \epsilon^{i-2}v_{ki} + \ldots + \epsilon^{n-2}v_{kn}$. After some algebra, the odd series coefficients for the horizontal reaction $h_{k[n]}$ read

$$h_{k1} = \frac{\cos\vartheta}{4\Lambda_d\delta_{k1}} \tag{61}$$

$$h_{k3} = -\left[\frac{\Lambda_2}{\Lambda_d} + \frac{\delta_{k3}}{\delta_{k1}}\right]\frac{\cos\vartheta}{4\Lambda_d\delta_{k1}} \tag{62}$$

$$h_{k5} = \left[\frac{\Lambda_2^2}{\Lambda_d^2} + \frac{\delta_{k3}\Lambda_2}{\delta_{k1}\Lambda_d} + \frac{\delta_{k3}^2}{\delta_{k1}^2} - \frac{\delta_{k5}}{\delta_{k1}}\right]\frac{\cos\vartheta}{4\Lambda_d\delta_{k1}} \tag{63}$$

while the even coefficients $h_{k2}, h_{k4}, \dots$ are found to be systematically null. Similarly, the odd series coefficients for the vertical reaction $v_{k[n]}$ read

$$v_{k1} = \frac{\varphi_{k0}\cos\vartheta}{4\Lambda_d\delta_{k1}} \tag{64}$$

$$v_{k3} = \left[\varphi_{k2} - \frac{\varphi_{k0}\delta_{k3}}{\delta_{k1}} - \frac{\varphi_{k0}\Lambda_2}{\Lambda_d}\right]\frac{\cos\vartheta}{4\Lambda_d\delta_{k1}} \tag{65}$$

$$v_{k5} = \left[\varphi_{k4} - \frac{\varphi_{k0}\delta_{k5} + \varphi_{k2}\delta_{k3}}{\delta_{k1}} + \frac{\varphi_{k0}\delta_{k3}^2}{\delta_{k1}^2} - \frac{\varphi_{k2}\Lambda_2}{\Lambda_d} + \frac{\varphi_{k0}\Lambda_2^2}{\Lambda_d^2} + \frac{\varphi_{k0}\delta_{k3}\Lambda_2}{\delta_{k1}\Lambda_d}\right]\frac{\cos\vartheta}{4\Lambda_d\delta_{k1}} \tag{66}$$

while, after substitution, it can be demonstrated that the first even coefficient $v_{k2}$ is unitary, whereas the higher even coefficients $v_{k4}, v_{k6}, \dots$ are null. It may be worth noting that the expressions (61)-(66) are formally similar to expressions (29)-(34), except for the relevant effects of the different consistency conditions.

To recap, the perturbation strategy provides fully analytical – although expressed in asymptotic form – functions $h_{k[n]} = \mathfrak{h}_k(\boldsymbol{x})$ and $v_{k[n]} = \mathfrak{v}_k(\boldsymbol{x})$ governing the nonlinear relation between the support reactions and the boundary displacements $\boldsymbol{x}$. According to the mainstream algorithmic strategy, the functions $\mathfrak{h}_k(\boldsymbol{x})$ and $\mathfrak{v}_k(\boldsymbol{x})$ can profitably be employed to asymptotically express the stiffness coefficients $\mathbf{k}_h$ and $\mathbf{k}_v$ governing the linear (exact) relations $dh = \mathbf{k}_h\, d\boldsymbol{x}$ and $dv = \mathbf{k}_v\, d\boldsymbol{x}$, by leveraging the formal analogy with the analytically determinable differentials $dh = \nabla\mathfrak{h}_k\, d\boldsymbol{x}$ and $dv = \nabla\mathfrak{v}_k\, d\boldsymbol{x}$, evaluated at $\boldsymbol{x} = \mathbf{0}$. As convenient algorithmic alternative, a lighter three-step procedure, that does not require the asymptotic expressions of the support reactions $h_{k[n]}$ and $v_{k[n]}$, can be pursued. As first step, the nonlinear formulas for the support reactions and the properties of derivatives can be used to express the *exact* gradient column vectors $\nabla\mathfrak{f}_k(\boldsymbol{x})$ and $\nabla\mathfrak{g}_k(\boldsymbol{x})$ (evaluated at $\boldsymbol{x} = \mathbf{0}$) in the form

$$\left[\nabla\mathfrak{f}_k(\boldsymbol{x})\right]_{\boldsymbol{x}=\mathbf{0}} = -\frac{\cos\vartheta}{4\,(\Lambda^\circ\,\delta^\circ)^2}\left[\nabla\Big(\Lambda(\boldsymbol{x})\delta_k(\boldsymbol{x})\Big)\right]_{\boldsymbol{x}=\mathbf{0}} \tag{67}$$

$$\left[\nabla\mathfrak{g}_k(\boldsymbol{x})\right]_{\boldsymbol{x}=\mathbf{0}} = -\frac{\varphi\cos\vartheta}{4\,(\Lambda^\circ\,\delta^\circ)^2}\left[\nabla\Big(\Lambda(\boldsymbol{x})\delta_k(\boldsymbol{x})\Big)\right]_{\boldsymbol{x}=\mathbf{0}} + \frac{\cos\vartheta}{4\,(\Lambda^\circ\,\delta^\circ)}\left[\nabla\varphi_k(\boldsymbol{x})\right]_{\boldsymbol{x}=\mathbf{0}} \tag{68}$$

where the dependence of the hyperstatic unknown $\delta(\boldsymbol{x})$, the function $\varphi(\boldsymbol{x})$ and, remarkably, the aspect ratio $\Lambda(\boldsymbol{x})$ (according to the extra-length expression $\Lambda(\boldsymbol{x}) = \Lambda_d(\boldsymbol{x}) + \Lambda_2$) on the boundary displacements $\boldsymbol{x}$ has been highlighted. Superscript $^\circ$ indicates evaluation at $\boldsymbol{x} = \mathbf{0}$ and, by recalling the solution of the problem for fixed supports, the noteworthy identities $\Lambda^\circ = [\Lambda(\boldsymbol{x})]_{\boldsymbol{x}=\mathbf{0}} = 1 + \Lambda_2 = \Lambda$ (aspect ratio), $\delta^\circ = [\delta_k(\boldsymbol{x})]_{\boldsymbol{x}=\mathbf{0}} = \delta$ (hyperstatic unknown) and $\varphi^\circ = [\varphi(\boldsymbol{x})]_{\boldsymbol{x}=\mathbf{0}} = \varphi$ can be recognized. From the mathematical viewpoint, it is interesting to remark that the gradients $\nabla\mathfrak{f}_k(\boldsymbol{x})$ and $\nabla\mathfrak{g}_k(\boldsymbol{x})$ depend on the product $\Gamma_k(\boldsymbol{x}) = \Lambda(\boldsymbol{x})\delta_k(\boldsymbol{x})$ and its derivatives, whereas they are independent of its factors (individually).

Based on the above considerations, the second step consists in asymptotically expressing the gradient vectors $\boldsymbol{\gamma}_k(\boldsymbol{x}) = \nabla\Gamma_k(\boldsymbol{x})$ and $\boldsymbol{\varphi}_k(\boldsymbol{x}) = \nabla\varphi_k(\boldsymbol{x})$. Recalling the consistency condition $\Lambda(\boldsymbol{x}) = \Lambda_d(\boldsymbol{x}) + \epsilon^2\Lambda_2$ for the aspect ratio and the expression $\delta_{k[n]}(\boldsymbol{x})$ of the hyperstatic unknown, after some algebra the product $\Gamma_k(\boldsymbol{x})$ turns out to have the asymptotic form $\Gamma_{k[n]}(\boldsymbol{x}) = \epsilon^1\Gamma_{k1}(\boldsymbol{x}) + \epsilon^2\Gamma_{k2}(\boldsymbol{x}) + \dots + \epsilon^i\Gamma_{ki}(\boldsymbol{x}) + \dots + \epsilon^n\Gamma_{kn}(\boldsymbol{x})$, where the odd series coefficients are

$$\Gamma_{k1}(\boldsymbol{x}) = \Lambda_d(\boldsymbol{x})\delta_{k1}(\boldsymbol{x}) \tag{69}$$

$$\Gamma_{k3}(\boldsymbol{x}) = \Lambda_d(\boldsymbol{x})\delta_{k3}(\boldsymbol{x}) + \Lambda_2\delta_{k1}(\boldsymbol{x}) \tag{70}$$

$$\Gamma_{k5}(\boldsymbol{x}) = \Lambda_d(\boldsymbol{x})\delta_{k5}(\boldsymbol{x}) + \Lambda_2\delta_{k3}(\boldsymbol{x}) \tag{71}$$

while the even coefficients $\Gamma_{k2}(\boldsymbol{x}), \Gamma_{k4}(\boldsymbol{x}), \Gamma_{k6}(\boldsymbol{x}), \dots$ are systematically null by construction. After differentiation and evaluation at $\boldsymbol{x} = \mathbf{0}$, the vector quantity $\boldsymbol{\gamma}_k^\circ = [\nabla\Gamma_k(\boldsymbol{x})]_{\boldsymbol{x}=\mathbf{0}}$ have the asymptotic expression $\boldsymbol{\gamma}_{k[n]}^\circ = \epsilon^{-1}\boldsymbol{\gamma}_{k1}^\circ + \epsilon^0\boldsymbol{\gamma}_{k2}^\circ + \dots + \epsilon^{i-2}\boldsymbol{\gamma}_{ki}^\circ + \dots + \epsilon^{n-2}\boldsymbol{\gamma}_{kn}^\circ$, where the odd series coefficients read in component form after reconstruction

$$\boldsymbol{\gamma}_{k1}^\circ = \frac{\Lambda_1}{8\Lambda_2}\left(\gamma_{11}^\circ, \gamma_{12}^\circ, \gamma_{13}^\circ, \gamma_{14}^\circ\right) \tag{72}$$

$$\boldsymbol{\gamma}_{k3}^\circ = \frac{\Lambda_1}{160\cos\vartheta}\left(\gamma_{31}^\circ, \gamma_{32}^\circ, \gamma_{33}^\circ, \gamma_{34}^\circ\right) \tag{73}$$

$$\boldsymbol{\gamma}_{k5}^\circ = \frac{\Lambda_1\Lambda_2}{8960\cos^3\vartheta}\left(\gamma_{51}^\circ, \gamma_{52}^\circ, \gamma_{53}^\circ, \gamma_{54}^\circ\right) \tag{74}$$

while the even coefficients $\boldsymbol{\gamma}_{k2}^\circ, \boldsymbol{\gamma}_{k4}^\circ, \boldsymbol{\gamma}_{k6}^\circ, \dots$ are systematically null by construction. The symmetries $\gamma_{i1}^\circ = -\gamma_{i3}^\circ$ and $\gamma_{i2}^\circ = -\gamma_{i4}^\circ$ hold (for all $i = 1, 3, 5, \dots$). The auxiliary quantities $\gamma_{ij}^\circ$ (for $j = 1, 2, 3, 4$) are reported in the Appendix A. Similarly, after cumbersome algebra the vector quantity $\boldsymbol{\varphi}_k^\circ = [\nabla\varphi_k(\boldsymbol{x})]_{\boldsymbol{x}=\mathbf{0}}$ is found to have the asymptotic expression $\boldsymbol{\varphi}_{k[n]}^\circ = \epsilon^{-1}\boldsymbol{\varphi}_{k1}^\circ + \epsilon^0\boldsymbol{\varphi}_{k2}^\circ + \dots + \epsilon^{i-2}\boldsymbol{\varphi}_{ki}^\circ + \dots + \epsilon^{n-2}\boldsymbol{\varphi}_{kn}^\circ$.

The series coefficients read

$$\boldsymbol{\varphi}^{\circ}_{k1}=\frac{\Lambda_1}{2\Lambda_2}\left(\varphi^{\circ}_{11},\varphi^{\circ}_{12},\varphi^{\circ}_{13},\varphi^{\circ}_{14}\right),\qquad \boldsymbol{\varphi}^{\circ}_{k2}=\frac{\sin\vartheta}{\cos\vartheta}\left(\varphi^{\circ}_{21},\varphi^{\circ}_{22},\varphi^{\circ}_{23},\varphi^{\circ}_{24}\right)\qquad \boldsymbol{\varphi}^{\circ}_{k3}=\frac{\Lambda_1}{40\cos^2\vartheta}\left(\varphi^{\circ}_{31},\varphi^{\circ}_{32},\varphi^{\circ}_{33},\varphi^{\circ}_{34}\right), \tag{75}$$

$$\boldsymbol{\varphi}^{\circ}_{k4}=\frac{2\Lambda_2}{5\cos^2\vartheta}\left(\varphi^{\circ}_{41},\varphi^{\circ}_{42},\varphi^{\circ}_{43},\varphi^{\circ}_{44}\right),\qquad \boldsymbol{\varphi}^{\circ}_{k5}=\frac{\Lambda_1\Lambda_2}{2560\cos^4\vartheta}\left(\varphi^{\circ}_{51},\varphi^{\circ}_{52},\varphi^{\circ}_{53},\varphi^{\circ}_{54}\right),\qquad \boldsymbol{\varphi}^{\circ}_{k6}=\frac{\Lambda_2^2}{700\cos^5\vartheta}\left(\varphi^{\circ}_{61},\varphi^{\circ}_{62},\varphi^{\circ}_{63},\varphi^{\circ}_{64}\right) \tag{76}$$

while the symmetries $\varphi^{\circ}_{i1}=-\varphi^{\circ}_{i3}$ and $\varphi^{\circ}_{i2}=-\varphi^{\circ}_{i4}$ hold (for all $i=1,2,3,...$). The auxiliary quantities $\varphi^{\circ}_{ij}$ (for $j=1,2,3,4$) are reported in the Appendix A. From the methodological viewpoint, it is important to remark that the differentiation causes a significant change in the asymptotic $\epsilon$-ordering, so that $\Gamma_{ki}(\boldsymbol{x}),\varphi_{ki}(\boldsymbol{x})\in\mathcal{O}(\epsilon^i)$ while $\|\boldsymbol{\gamma}^{\circ}_{ki}\|,\|\boldsymbol{\varphi}^{\circ}_{ki}\|\in\mathcal{O}(\epsilon^{i-2})$, because $\boldsymbol{\gamma}^{\circ}_{ki}\neq[\nabla\Gamma_{ki}(\boldsymbol{x})]_{\boldsymbol{x}=\boldsymbol{0}}$ and $\boldsymbol{\varphi}^{\circ}_{ki}\neq[\nabla\varphi_{ki}(\boldsymbol{x})]_{\boldsymbol{x}=\boldsymbol{0}}$, according to a consistent perturbation scheme.

Considering the formal analogy between the stiffness row matrices $\mathbf{k}_h$, $\mathbf{k}_v$ and the gradient vectors $\left[\nabla\mathfrak{f}_k(\boldsymbol{x})\right]_{\boldsymbol{x}=\boldsymbol{0}}$, $\left[\nabla\mathfrak{g}_k(\boldsymbol{x})\right]_{\boldsymbol{x}=\boldsymbol{0}}$ for the horizontal and vertical reaction, the asymptotic expression of the row matrices is found in the form $\mathbf{k}_{h[n]}=\epsilon^{-3}\mathbf{k}_{h1}+\epsilon^{-2}\mathbf{k}_{h2}+...+\epsilon^{i-4}\mathbf{k}_{hi}+...+\epsilon^{n-4}\mathbf{k}_{hn}$ (for the horizontal reaction) and $\mathbf{k}_{v[n]}=\epsilon^{-3}\mathbf{k}_{v1}+\epsilon^{-2}\mathbf{k}_{v2}+...+\epsilon^{i-4}\mathbf{k}_{vi}+...+\epsilon^{n-4}\mathbf{k}_{vn}$ (for the vertical reaction). It is important to note that – consistently with the perturbation scheme – the $i$-th terms $\mathbf{k}_{hi}$ and $\mathbf{k}_{vi}$ of the stiffness series belong to the $(i-4)$-th order $\mathcal{O}(\epsilon^{i-4})$ and, consequently, the lowest-order stiffness approximation $\|\mathbf{k}_{h1}\|\in\mathcal{O}(\epsilon^{-3})$. Physically, this mathematical result formalizes the mechanical concept that the horizontal and vertical reactions are extremely sensitive to small support displacements. First, by introducing in equation (67) the asymptotic expressions $\delta_{k[n]}$ and $\boldsymbol{\gamma}^{\circ}_{k[n]}$ and taking also into account the consistency condition $\Lambda=1+\epsilon^2\Lambda_2$, the odd series coefficients of the asymptotic row matrix $\mathbf{k}_{h[n]}$ read

$$\mathbf{k}_{h1}=-\frac{\cos\vartheta}{4\delta_{k1}^2}\,\boldsymbol{\gamma}^{\circ}_{k1} \tag{77}$$

$$\mathbf{k}_{h3}=-\frac{\cos\vartheta}{4\delta_{k1}^2}\left[\boldsymbol{\gamma}^{\circ}_{k3}-2\Lambda_2\boldsymbol{\gamma}^{\circ}_{k1}-\frac{2\delta_{k3}\boldsymbol{\gamma}^{\circ}_{k1}}{\delta_{k1}}\right] \tag{78}$$

$$\mathbf{k}_{h5}=-\frac{\cos\vartheta}{4\delta_{k1}^2}\left[\boldsymbol{\gamma}^{\circ}_{k5}-2\Lambda_2\boldsymbol{\gamma}^{\circ}_{k3}+3\Lambda_2^2\boldsymbol{\gamma}^{\circ}_{k1}+\frac{2(\delta_{k3}(2\Lambda_2\boldsymbol{\gamma}^{\circ}_{k1}-\boldsymbol{\gamma}^{\circ}_{k3})-\delta_{k5}\boldsymbol{\gamma}^{\circ}_{k1})}{\delta_{k1}}+\frac{3\delta_{k3}^2\boldsymbol{\gamma}^{\circ}_{k1}}{\delta_{k1}^2}\right] \tag{79}$$

while the even coefficients $\mathbf{k}_{h2},\mathbf{k}_{h4},\mathbf{k}_{h6},...$ are systematically null by construction. Second, by introducing in equation (68) the asymptotic expressions $\delta_{k[n]}$, $\boldsymbol{\gamma}^{\circ}_{k[n]}$, $\boldsymbol{\varphi}^{\circ}_{k[n]}$ and taking also into account the consistency condition $\Lambda=1+\epsilon^2\Lambda_2$, the series coefficients of the asymptotic row matrix $\mathbf{k}_{v[n]}$ read

$$\mathbf{k}_{v1}=-\frac{\cos\vartheta}{4\delta_{k1}^2}\,\varphi_{k0}\boldsymbol{\gamma}^{\circ}_{k1} \tag{80}$$

$$\mathbf{k}_{v2}=-\frac{\cos\vartheta}{4\delta_{k1}^2}\,\varphi_{k1}\boldsymbol{\gamma}^{\circ}_{k1}+\frac{\cos\vartheta}{4\delta_{k1}}\,\boldsymbol{\varphi}^{\circ}_{k1} \tag{81}$$

$$\mathbf{k}_{v3}=-\frac{\cos\vartheta}{4\delta_{k1}^2}\left[\varphi_{k2}\boldsymbol{\gamma}^{\circ}_{k1}+\varphi_{k0}\boldsymbol{\gamma}^{\circ}_{k3}-2\Lambda_2\varphi_{k0}\boldsymbol{\gamma}^{\circ}_{k1}-\frac{2\delta_{k3}\varphi_{k0}\boldsymbol{\gamma}^{\circ}_{k1}}{\delta_{k1}}\right]+\frac{\cos\vartheta}{4\delta_{k1}}\,\boldsymbol{\varphi}^{\circ}_{k2} \tag{82}$$

$$\mathbf{k}_{v4}=-\frac{\cos\vartheta}{4\delta_{k1}^2}\left[\varphi_{k3}\boldsymbol{\gamma}^{\circ}_{k1}+\varphi_{k1}\boldsymbol{\gamma}^{\circ}_{k3}-2\Lambda_2\varphi_{k1}\boldsymbol{\gamma}^{\circ}_{k1}-\frac{2\delta_{k3}\varphi_{k1}\boldsymbol{\gamma}^{\circ}_{k1}}{\delta_{k1}}\right]+\frac{\cos\vartheta}{4\delta_{k1}}\left[\boldsymbol{\varphi}^{\circ}_{k3}-\Lambda_2\boldsymbol{\varphi}^{\circ}_{k1}-\frac{\delta_{k3}\boldsymbol{\varphi}^{\circ}_{k1}}{\delta_{k1}}\right] \tag{83}$$

$$\begin{aligned}\mathbf{k}_{v5}=&-\frac{\cos\vartheta}{4\delta_{k1}^2}\left[\varphi_{k4}\boldsymbol{\gamma}^{\circ}_{k1}+\varphi_{k2}\boldsymbol{\gamma}^{\circ}_{k3}+\varphi_{k0}\boldsymbol{\gamma}^{\circ}_{k5}-2\Lambda_2\varphi_{k2}\boldsymbol{\gamma}^{\circ}_{k1}-2\Lambda_2\varphi_{k0}\boldsymbol{\gamma}^{\circ}_{k3}+3\Lambda_2^2\varphi_{k0}\boldsymbol{\gamma}^{\circ}_{k1}\right]+\\&+\frac{\cos\vartheta}{4\delta_{k1}^2}\left[\frac{2\delta_{k3}\varphi_{k0}\boldsymbol{\gamma}^{\circ}_{k3}}{\delta_{k1}}+\frac{2\delta_{k3}\varphi_{k2}\boldsymbol{\gamma}^{\circ}_{k1}}{\delta_{k1}}+\frac{2\delta_{k5}\varphi_{k0}\boldsymbol{\gamma}^{\circ}_{k1}}{\delta_{k1}}-\frac{4\Lambda_2\varphi_{k0}\delta_{k3}\boldsymbol{\gamma}^{\circ}_{k1}}{\delta_{k1}}-\frac{3\delta_{k3}^2\varphi_{k0}\boldsymbol{\gamma}^{\circ}_{k1}}{\delta_{k1}^2}\right]+\\&+\frac{\cos\vartheta}{4\delta_{k1}}\left[\boldsymbol{\varphi}^{\circ}_{k4}-\Lambda_2\boldsymbol{\varphi}^{\circ}_{k2}-\frac{\delta_{k3}\boldsymbol{\varphi}^{\circ}_{k2}}{\delta_{k1}}\right]\end{aligned} \tag{84}$$

$$\begin{aligned}\mathbf{k}_{v6}=&-\frac{\cos\vartheta}{4\delta_{k1}^2}\left[\varphi_{k5}\boldsymbol{\gamma}^{\circ}_{k1}+\varphi_{k3}\boldsymbol{\gamma}^{\circ}_{k3}+\varphi_{k1}\boldsymbol{\gamma}^{\circ}_{k5}-2\Lambda_2\varphi_{k3}\boldsymbol{\gamma}^{\circ}_{k1}-2\Lambda_2\varphi_{k1}\boldsymbol{\gamma}^{\circ}_{k3}+3\Lambda_2^2\varphi_{k1}\boldsymbol{\gamma}^{\circ}_{k1}\right]+\\&+\frac{\cos\vartheta}{4\delta_{k1}^2}\left[\frac{2\delta_{k3}\varphi_{k1}\boldsymbol{\gamma}^{\circ}_{k3}}{\delta_{k1}}+\frac{2\delta_{k3}\varphi_{k3}\boldsymbol{\gamma}^{\circ}_{k1}}{\delta_{k1}}+\frac{2\delta_{k5}\varphi_{k1}\boldsymbol{\gamma}^{\circ}_{k1}}{\delta_{k1}}-\frac{4\Lambda_2\varphi_{k1}\delta_{k3}\boldsymbol{\gamma}^{\circ}_{k1}}{\delta_{k1}}-\frac{3\delta_{k3}^2\varphi_{k1}\boldsymbol{\gamma}^{\circ}_{k1}}{\delta_{k1}^2}\right]+\\&+\frac{\cos\vartheta}{4\delta_{k1}}\left[\boldsymbol{\varphi}^{\circ}_{k5}-\Lambda_2\boldsymbol{\varphi}^{\circ}_{k3}+\Lambda_2^2\boldsymbol{\varphi}^{\circ}_{k1}-\frac{\delta_{k5}\boldsymbol{\varphi}^{\circ}_{k1}}{\delta_{k1}}-\frac{\delta_{k3}\boldsymbol{\varphi}^{\circ}_{k3}}{\delta_{k1}}+\frac{\Lambda_2\delta_{k3}\boldsymbol{\varphi}^{\circ}_{k1}}{\delta_{k1}}+\frac{\delta_{k3}^2\boldsymbol{\varphi}^{\circ}_{k1}}{\delta_{k1}^2}\right]\end{aligned} \tag{85}$$

where the even coefficients $\mathbf{k}_{v2},\mathbf{k}_{v4},\mathbf{k}_{v6},...$ are systematically null by demonstration. It is worth noting that the $i$-the series coefficient $\mathbf{k}_{vi}$ depends on the $i$-th series term $\boldsymbol{\gamma}^{\circ}_{ki}$ and the $(i-1)$-th series term $\boldsymbol{\varphi}^{\circ}_{k(i-1)}$. Physically, this mathematical result indicates that small changes in the inclination angle can influence the vertical reaction sensitivity more strongly than small changes in the aspect ratio.

Coherently with the symmetry properties of the exact stiffness coefficients, the component form of the asymptotic row matrices $\mathbf{k}_{h[n]} = \left(k^h_{xA[n]}, k^h_{yA[n]}, k^h_{xB[n]}, k^h_{yB[n]}\right)$ and $\mathbf{k}_{v[n]} = \left(k^v_{xA[n]}, k^v_{yA[n]}, k^v_{xB[n]}, k^v_{yB[n]}\right)$ can be demonstrated to respect the symmetry relations

$$k^h_{x[n]} := k^h_{xB[n]} = -k^h_{xA[n]}, \qquad k^h_{y[n]} := k^h_{yB[n]} = -k^h_{yA[n]} \tag{86}$$

$$k^v_{x[n]} := k^v_{xB[n]} = -k^v_{xA[n]}, \qquad k^v_{y[n]} := k^v_{yB[n]} = -k^v_{yA[n]} \tag{87}$$

after differentiation and reconstruction. By virtue of the symmetries, the catenary stiffness matrix $\mathbf{K}$ can be asymptotically expressed in the form $\mathbf{K}_{[n]} = \epsilon^{-3}\mathbf{K}_1 + \epsilon^{-1}\mathbf{K}_3 + \ldots + \epsilon^{i-4}\mathbf{K}_i + \ldots + \epsilon^{n-4}\mathbf{K}_n$ (with $i, n$ even) according to its definition (44), yielding

$$\mathbf{K}_{[n]} = \mathbf{R}\begin{pmatrix} \mathbf{k}_{h[n]} \\ \mathbf{k}_{v[n]} \end{pmatrix}\mathbf{S} = \begin{pmatrix} k^h_{x[n]} & -k^h_{y[n]} & -k^h_{x[n]} & k^h_{y[n]} \\ -k^v_{x[n]} & k^v_{y[n]} & k^v_{x[n]} & -k^v_{y[n]} \\ -k^h_{x[n]} & k^h_{y[n]} & k^h_{x[n]} & -k^h_{y[n]} \\ k^v_{x[n]} & -k^v_{y[n]} & -k^v_{x[n]} & k^v_{y[n]} \end{pmatrix} \tag{88}$$

where the coefficients have the asymptotic expressions $k^h_{x[n]} = \epsilon^{-3}k^h_{x1} + \epsilon^{-1}k^h_{x3} + \ldots + \epsilon^{i-4}k^h_{xi} + \ldots + \epsilon^{n-4}k^h_{xn}$, $k^h_{y[n]} = \epsilon^{-3}k^h_{y1} + \epsilon^{-1}k^h_{y3} + \ldots + \epsilon^{i-4}k^h_{yi} + \ldots + \epsilon^{n-4}k^h_{yn}$, $k^v_{x[n]} = \epsilon^{-3}k^v_{x1} + \epsilon^{-1}k^v_{x3} + \ldots + \epsilon^{i-4}k^v_{xi} + \ldots + \epsilon^{n-4}k^v_{xn}$, $k^v_{y[n]} = \epsilon^{-3}k^v_{y1} + \epsilon^{-1}k^v_{y3} + \ldots + \epsilon^{i-4}k^v_{yi} + \ldots + \epsilon^{n-4}k^v_{yn}$ (with $i, n$ even). Remarkably, it can be demonstrated that $k^h_{yi} = k^v_{xi}$ for $i = 1, 3, 5, \ldots$. This identity suffices to prove that $\mathbf{K}_i = \mathbf{K}_i^\top$, meaning that the symmetry of the stiffness matrix holds *at each order*, ensuring the possibility to achieve consistent asymptotic approximations (by truncating the series), without violating physical requirements.

In conclusion, as major physical-mathematical achievement, the semi-analytical catenary stiffness matrix $\mathbf{K}$ is asymptotically determined as a known analytical – although asymptotically approximate – function $\mathbf{K}_{[n]}(\Lambda, \vartheta)$ of the aspect ratio $\Lambda$ and the inclination angle $\vartheta$. Due to its geometric nature, the stiffness matrix certainly depends on the cable tension (through the hyperstatic unknown). This fundamental dependence is conveniently integrated by leveraging the analytical tension-to-parameter relation satisfying automatically the compatibility condition (in a suited asymptotic sense). After substitutions and reconstruction (for $n = 6$), ready-to-use and relatively simple expressions can be achieved for the independent stiffness coefficients

$$\begin{aligned}
k^h_{x[6]} &= \frac{\cos^4\vartheta}{2\Lambda_1(\Lambda-1)} + \frac{(109 - 35\cos(2\vartheta))\cos^2\vartheta}{80\Lambda_1} - \frac{\Lambda_1(6561 + 10220\cos(2\vartheta) - 2485\cos(4\vartheta))}{107520} \\
k^h_{y[6]} = k^v_{x[6]} &= \frac{\sin\vartheta\cos^3\vartheta}{2\Lambda_1(\Lambda-1)} - \frac{(51 + 35\cos(2\vartheta))\sin\vartheta\cos\vartheta}{80\Lambda_1} + \frac{\Lambda_1(15839 + 12180\cos(2\vartheta) + 2485\cos(4\vartheta))\sin\vartheta}{107520\cos\vartheta} \\
k^v_{y[6]} &= \frac{\sin^2\vartheta\cos^2\vartheta}{2\Lambda_1(\Lambda-1)} + \frac{80 - (211 + 35\cos(2\vartheta))\sin^2\vartheta}{80\Lambda_1} + \frac{\Lambda_1\left(20608 + (60639 + 34580\cos(2\vartheta) + 2485\cos(4\vartheta))\sin^2\vartheta\right)}{107520\cos^2\vartheta}
\end{aligned} \tag{89}$$

where the (reconstructed) auxiliary quantity $\Lambda_1 = [6(\Lambda-1)]^{1/2}$. The corresponding dimensional stiffness coefficients are obtained by multiplying by the dimensional reference stiffness $k_0 = \frac{1}{2}w\Lambda\sec\vartheta$.

Parametric analyses comparing the exact stiffness coefficients $k^h_x$, $k^v_y$, $k^h_y$ (black dots) versus asymptotic approximations $k^h_{x[n]}, k^v_{y[n]}, k^h_{y[n]}$ over the technically relevant range of the mechanical parameters $(\vartheta, \Lambda)$ are illustrated in Fig. 7 for high approximation orders ($n = 6$). Generally, the largest values of all the stiffness coefficients are associated to lower values of the aspect ratios $\Lambda$ (Fig. 7a,c,e), as expected. From the quantitative viewpoint, the comparison shows that the asymptotic approximations achieve satisfying levels of agreement with the exact stiffness coefficients, with extremely low errors for $k^h_x$ (namely absolute values of $e^h_x = (k^h_{x[6]} - k^h_x)/k^h_x$ lower than $8\times10^{-5}$, see Fig. 7b) and very low errors for $k^v_y$ (absolute values of $e^v_y = (k^v_{y[6]} - k^v_y)/k^v_y$ lower than $5\times10^{-3}$, see Fig. 7d) and for $k^h_y$ (absolute values of $e^h_y = (k^h_{y[6]} - k^h_y)/k^h_y$ lower than $5\times10^{-4}$, see Fig. 7f). From the qualitative viewpoint, it can be remarked that the asymptotic approximation $k^h_{x[6]}$ underestimates the exact coefficients $k^h_x$, while the asymptotic approximations $k^v_{y[6]}$ and $k^h_{y[6]}$ overestimates the exact coefficients $k^v_y$ and $k^h_y$ over the full range of mechanical parameters.

## 4. A paradigmatic application: the catenary cable-stayed beam

The cable-stayed beam is a minimal reference model, widely recognized as paradigmatic structural system for studying the beam-cable collaborations characterizing a variety of cable structures. Different mechanical formulations of the cable-stayed beam model have been employed in the literature to study linear and nonlinear dynamic phenomena [38–41] and vibration control strategies [32,42–45]. Consequently, the cable-stayed beam composed by a slender horizontal cantilever, supported at the free end by an inclined inextensible cable is selected as benchmark to apply the asymptotic catenary solutions (Fig. 8). The beam is described as an unshearable, compressible, flexible and linearly elastic one-dimensional continuum. According to the assumptions, the beam is mechanically characterized by the natural length $L$, equal to the cable span, and the axial and flexural rigidities $EA_b$ and $EI_b$, respectively. The inextensible cable is characterized by the chord inclination angle $\vartheta$, the self-weight $w$ per unit length and the natural length $L_0$. The upper support of the cable is assumed fixed and exerts the unknown horizontal and vertical reactions $H$ and $V$, respectively (see also Fig. 1). A uniformly distributed transversal load $w_b$ is quasistatically applied (downward) all along the beam axis. The beam axis is spanned by the coordinate $X_b \in [0, L]$, which serves as independent variable for the unknown functions $U_b(X_b)$ and $V_b(X_b)$ describing the axial and transversal displacements, respectively. The cable configuration is described by the cartesian function $y(x)$.

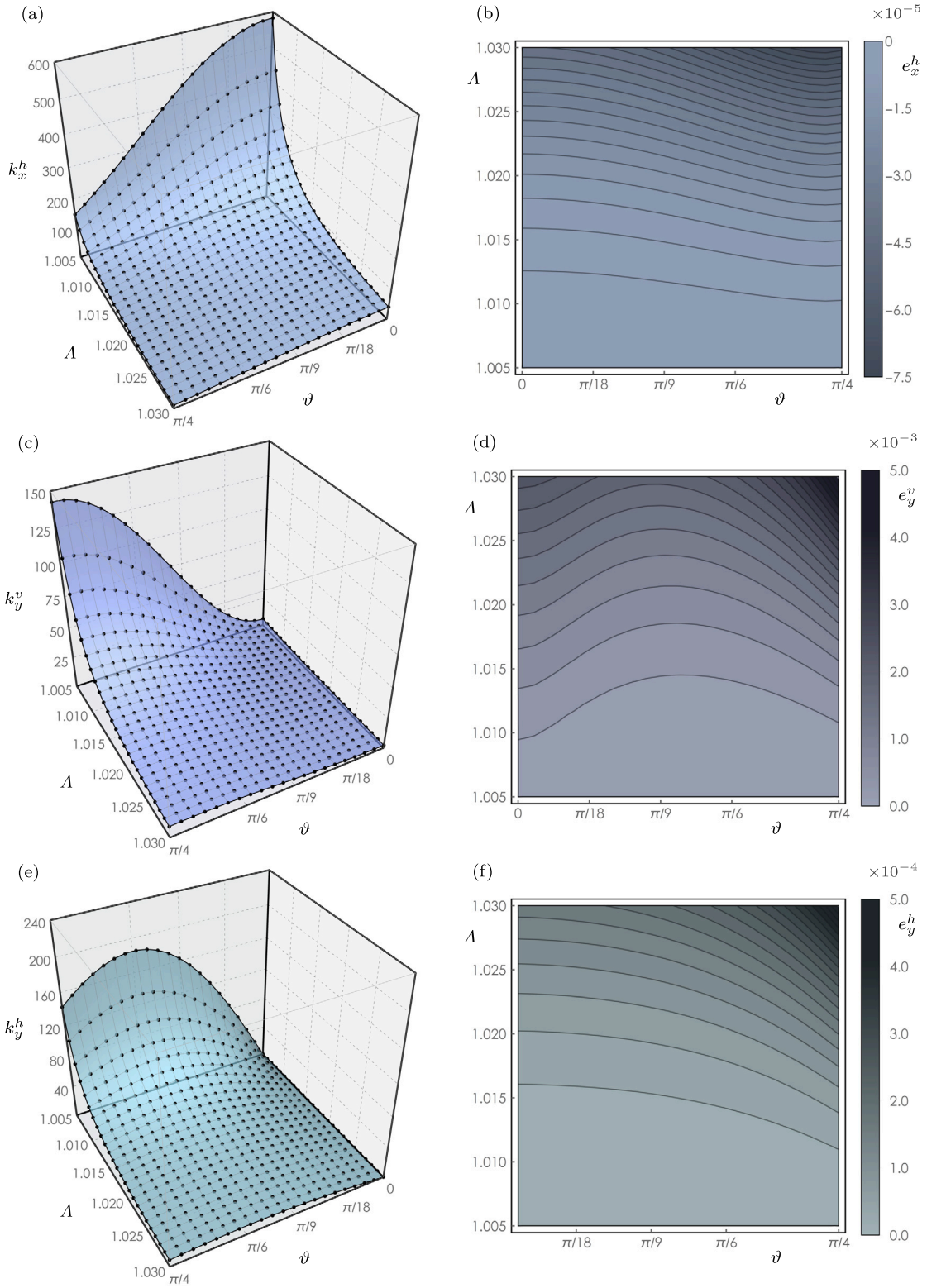


**Fig. 7.** Exact stiffness coefficients $k_x^h$, $k_y^v$, $k_y^h$ (black dots) versus asymptotic approximations $k_{x[6]}^h, k_{y[6]}^v, k_{y[6]}^h$ (surfaces) for varying mechanical parameters in the relevant range of aspect ratios $\Lambda \in [1005/1000, 1030/1000]$ and inclination angles $\vartheta \in [0, \pi/4]$: (a),(b) $k_x^h$ and $e_x^h$ (contour plot), (c),(d) $k_y^v$ and $e_y^v$ (contour plot), (e),(f) $k_y^h$ and $e_y^h$ (contour plot).

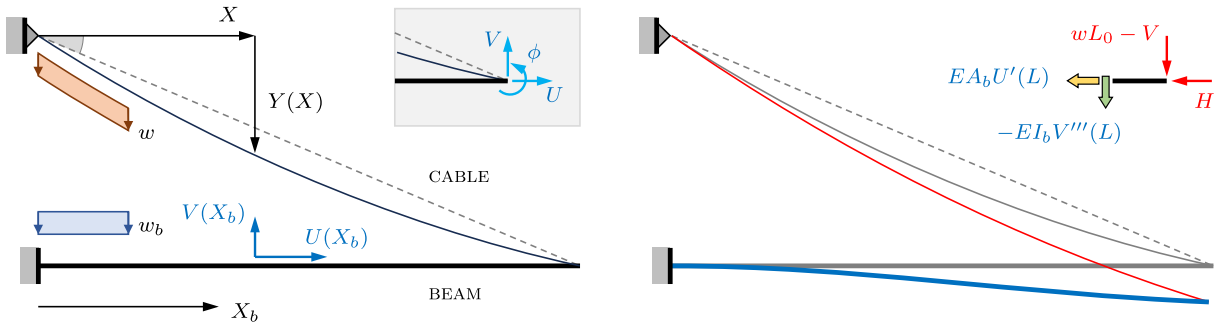


**Fig. 8.** Cable-stayed beam: configuration functions and nodal displacements (left), static equilibrium configuration (right).

The elastic problem consists in finding the static equilibrium configuration of the cable-stayed beam in the vertical plane under the concurrent effects of the cable self-weight $w$ and the beam load $w_b$. The compression force developed in the beam is assumed lower than the first critical load, so that the solution is expected to be unique (although a stability analysis for buckling could be performed straightforwardly with a minimal model enrichment). The problem is conveniently formulated in nondimensional terms by introducing dimensionless variables and parameters

$$x_b = \frac{X_b}{L}, \qquad u_b = \frac{U_b}{L}, \qquad v_b = \frac{V_b}{L}, \qquad p_c = \frac{wL_0}{2EA_b}, \qquad p_b = \frac{w_bL}{EA_b}, \qquad \varrho_b^2 = \frac{EI_b}{EA_bL^2} \tag{90}$$

where, from the physical viewpoint, the parameter $\varrho_b$ is the nondimensional radius of gyration of the beam cross section (also accounting for the inverse of the beam slenderness). The quantity $p_c/p_b$ expresses the ratio between the total loads acting on the cable and the beam, respectively. The dimensionless configuration variables $x = X/L$ and $y = Y/L$, reactions $h = (2H)/(wL_0)$ and $\nu = (2V)/(wL_0)$ are recalled for the cable. The aspect ratio $\Lambda = L_0/L\cos\vartheta$ will be also used.

The elastic problem is solved by means of two different strategies: (i) a *hybrid displacement-force method*, providing exact numerical results, taken as reference, and (ii) a high-order *asymptotic direct stiffness method*, providing numerical, but also analytical results if the direct stiffness method is applied in incremental form. The objective is to compare the asymptotic results with the exact results, for the largest order $n$.

### 4.1. Hybrid displacement-force method

A hybrid strategy based on the displacement method (for the beam) and the force method (for the cable) is developed. Considering first the beam, the linear differential equations governing the axial and transversal equilibrium are solved by imposing all the boundary conditions (see Appendix B for details). Specifically, by accounting for the hyperstatic unknowns $(h, \nu)$ in the equilibrium condition at the cable-beam joint (Fig. 8), the beam configuration is described by the displacement functions

$$u_b(x_b) = -\frac{\Lambda h p_c}{\cos\vartheta}x_b, \qquad v_b(x_b) = \frac{12\Lambda(\nu-2)p_c\sec\vartheta - 6p_b}{24\varrho_b^2}x_b^2 - \frac{4\Lambda(\nu-2)p_c\sec\vartheta - 4p_b}{24\varrho_b^2}x_b^3 - \frac{p_b}{24\varrho_b^2}x_b^4 \tag{91}$$

which describe all the statically determinable solutions for the beam, under variation of the hyperstatic unknowns $(h, \nu)$. The systematic shortening of the beam ($u_b(x_b) < 0$), due to the compressive horizontal force $h$ exerted by the cable, can be remarked. On the contrary, the beam can undergo positive bending ($v_b''(x_b) > 0$) or negative bending ($v_b''(x_b) < 0$), mainly depending on the ratio $p_c/p_b$. The equilibrium configuration of slender beams (characterized by very small values of the parameter $\varrho^2$) tends to be dominated by the vertical displacement $v_b(x_b)$, as expected.

The statically determinate solutions must satisfy the *kinematic compatibility conditions* $u_b(1) = x_B$ and $v_b(1) = -y_B$, coupling the beam displacements $u_b(1)$ and $v_b(1)$ with the cable displacements $x_B$ and $y_B$ at the beam-cable joint. Therefore, the kinematic compatibility conditions, together with the remaining boundary conditions $x_A = 0$ and $y_A = 0$, can be imposed into the catenary function (45) and arc-length (47) for the cable hanging between displaceable supports. Finally, the hyperstatic unknowns $(h, \nu)$ must satisfy the coupled system of nonlinear algebraic equations

$$\Lambda_k(h,\nu) = \Lambda, \qquad \Psi_k(h,\nu) = \operatorname{arcsinh}(\nu/h) \tag{92}$$

where the former equation is the compatibility (inextensibility) equation, while the latter is the hyperstatic relation. The nondimensional functions at the left-hand are

$$\Lambda_k(h,\nu) = h\Lambda\sinh\left(\frac{\cos\vartheta}{h\Lambda} - p_c\right)\cosh\left(\Psi_k(h,\nu) + p_c - \frac{\cos\vartheta}{h\Lambda}\right) \tag{93}$$

$$\Psi_k(h,\nu) = \frac{\cos\vartheta}{\Lambda h} - p_c + \operatorname{arcsinh}\left[\Psi_b(h,\nu)\operatorname{csch}\left(p_c - \frac{\cos\vartheta}{\Lambda h}\right)\right] \tag{94}$$

where $\Psi_b(h,\nu) = \left[8\Lambda p_c(\nu-2) - 24\varrho_b^2\sin\vartheta - 3p_b\cos\vartheta\right]/(24\Lambda\varrho_b^2 h)$. The admissible (real-valued) solutions $h^*$ and $\nu^*$ cannot be determined analytically, and must be assessed numerically.

Once the hyperstatic unknowns have been assessed numerically, the problem solution describes the static equilibrium configuration for the cable $y^*(x)$ and the beam $u_b^*(x_b)$ and $v_b^*(x_b)$, together with the respective internal forces. The occurrence of positive bending for the beam (*uplift* phenomenon), caused by the strong tensions in short cables ($\Lambda$ close to unity) supporting slightly loaded beams (small $w_b$) is exactly describable. Furthermore, the quasi-perfect constraint (*locking* phenomenon) limiting the transversal displacements at the beam tip at the largest value compatible with the cable inextensibility, is also exactly describable (with extra loads mainly adsorbed by the axial compressibility of the beam).

### 4.2. Asymptotic direct stiffness method

As an alternative to the hybrid displacement-force method, it may be convenient to approach the static problem of the catenary cable-stayed beam by adopting an asymptotic direct stiffness method. The methodological advantage is twofold. First, outlining a systematic solution scheme for catenary cable-stayed structures in the framework of the direct stiffness technique has a natural computational convenience, since the method generates low-dimension models governed by algebraic equations. Second, combining the direct stiffness method with the asymptotic expressions of the catenary stiffness matrices provides linear (incremental) relations between nodal forces and displacements. Therefore, the inversion of such relations provides analytical functions suited to be implemented in parametric design strategies.

According to the direct stiffness method, the set of dimensionless nodal displacements $u$, $v$ and $\phi$ at the cable-beam joint can be assumed as kinematic unknowns (Fig. 8). In particular, the nodal displacements can be associated to the boundary displacements of the beam and the cable by the compatibility relations $u = u_b(1) = x_B$, $v = v_b(1) = -y_B$, $\phi = v_b'(1)$. By condensing the nodal rotation, which linearly depends on the transversal displacement according to the relation $\phi = 3/2\, v + 1/48\, p_b/\varrho_b^2$, the horizontal and vertical equilibrium at the cable-beam joint is governed by the coupled system of two nonlinear algebraic equations

$$u + \Lambda p_c \sec\vartheta\, h(u,v) = 0, \tag{95}$$

$$24\varrho_b^2 v - 8\,\Lambda p_c \sec\vartheta\, v(u,v) = -3p_b - 16\Lambda p_c \sec\vartheta \tag{96}$$

where, however, the exact functions $h(u,v)$ and $v(u,v)$ cannot be given in explicit analytical form. Consequently, the solutions cannot be achieved analytically, and remain also difficult to be assessed numerically.

The algorithmic bottleneck can be by-passed by invoking the asymptotic solutions for the catenary cable hanging between displaceable supports. Indeed, by recalling that the functions $h(u,v)$ and $v(u,v)$ can be expressed in the asymptotic form $h_{[n]}(u,v)$ and $v_{[n]}(u,v)$, the condensed coupled system of algebraic equations (95)-(96) can conveniently be imposed in the asymptotic form

$$u + \Lambda p_c \sec\vartheta\, h_{[n]}(u,v) = 0, \tag{97}$$

$$24\varrho_b^2 v - 8\,\Lambda p_c \sec\vartheta\, v_{[n]}(u,v) = -3p_b - 16\Lambda p_c \sec\vartheta \tag{98}$$

where $h_{[n]}(u,v)$ and $v_{[n]}(u,v)$ are nonlinear functions of the unknown nodal displacements defined for growing orders $n$, according to equations (61)-(63) and (64)-(66). Fixed a certain order $n$, the admissible solutions $u_{[n]}^*$ and $v_{[n]}^*$ can straightforwardly be achieved numerically. Being $n$ finite, the solutions are approximate.

The asymptotically approximate (numerical) solutions $u_{[n]}^*$ and $v_{[n]}^*$, assessed through the direct stiffness method, can be compared with the exact (numerical) solutions $u^*$ and $v^*$, assessed through the hybrid displacement-force method, are compared in Fig. 9. The quasistatic response of the catenary cable-stayed beam for growing loads $p_b$ is considered, by varying the aspect ratio $\Lambda$ of the cable to perform a significant parametric analysis. From the qualitative viewpoint, the results highlight the significant nonlinearity of the response for growing loads $p_b$. The nonlinear response has softening behavior for the $u$-variable (axial beam shortening) and hardening behavior for the $v$-variable (transversal beam deflection), as expected. From the quantitative viewpoint, the comparison shows that the high-order ($n = 6$) asymptotic solutions (pink surface for $u_{[6]}$ and purple surface for $v_{[6]}$) match the exact solutions (black dots for $u^* = u_b^*(1)$ and $v^* = v_b^*(1)$) with excellent agreement. The relevant phenomena of beam uplift (positive $v$-values for small loads $p_b$) and beam tip locking (reducing $v$-increments versus growing $u$-decrements for small beam loads $p_b$ and short cables $\Lambda \simeq 1$) are also well fitted. Specifically, the asymptotic response approximates the exact response with relative errors $e_s = |(s_{[6]} - s^*)/(\max(s) + s)|$ lower than $5 \times 10^{-6}$ over the full variation range of the beam load $p_b$ and the aspect ratio $\Lambda$ (see Fig. 7c). The quantity $s = (u^2 + v^2)^{1/2}$ indicates the amplitude of the total displacement at the cable-beam joint.

The methodological advantages of using the asymptotic direct stiffness method are even more evident if the static problem of the catenary cable-stayed beam is conveniently formulated in incremental terms. To this purpose, the static equilibrium configuration of the system with fixed nodes is taken as reference. Accordingly, the reference nodal displacements are null ($u^\circ = 0$, $v^\circ = 0$). The reference reactions ($h^\circ, v^\circ$) are not null and clearly coincide with the reactions of the catenary cable between fixed supports, which can be considered known numerically of analytically (in asymptotic form). Therefore, the final configuration is sought for by stating the governing equations (95)-(96) in the incremental form

$$(u^\circ + du) + \Lambda p_c \sec\vartheta\, h(u^\circ + du, v^\circ + dv) = 0, \tag{99}$$

$$24\varrho_b^2(v^\circ + dv) - 8\,\Lambda p_c \sec\vartheta\, v(u^\circ + du, v^\circ + dv) = -3p_b - 16\Lambda p_c \sec\vartheta \tag{100}$$

where, by recalling the equations (43) and imposing the kinematic compatibility relations, the incremented reactions can be expressed in the form $h(u^\circ + du, v^\circ + dv) = h(u^\circ, v^\circ) + k_x^h\, du - k_y^h\, dv = h^\circ + k_x^h\, du - k_y^h\, dv$ and $v(u^\circ + du, v^\circ + dv) = v(u^\circ, v^\circ) + k_x^v\, du - k_y^v\, dv =$

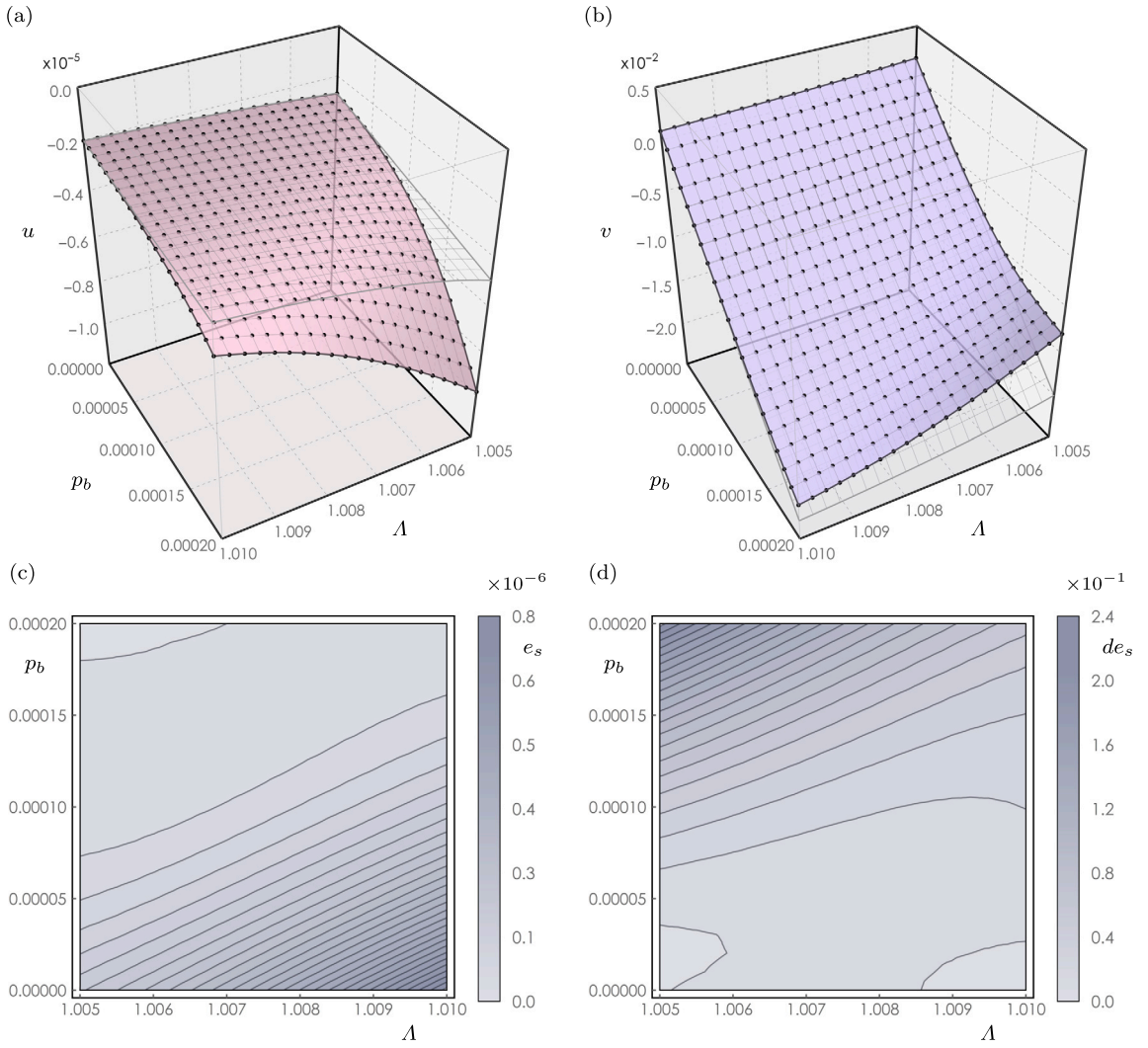


**Fig. 9.** Catenary cable-stayed beam response under increasing beam loads $p_b$ for different cable aspect ratios $\Lambda$ (with $\vartheta = \pi/8$, $\varrho_b^2 = 1/1000$, $p_c = 5\times10^{-6}$). Comparison of the numerical response determined according to the hybrid displacement-force method (black dots) versus the numerical response determined according to the asymptotic direct stiffness method (surfaces) and the analytical response determined according to the asymptotic incremental direct stiffness method (wireframes): (a),(b) nodal displacements $u$ (pink surface) and $v$ (purple surface), (c),(d) relative errors $e_s$ and $de_s$.

$\nu^\circ + k_x^v\,du - k_y^v\,dv$. The stiffness coefficients $k_x^h$, $k_y^h$, $k_x^v$, $k_y^v$ can be considered known numerically or analytically (in asymptotic form). Consequently, the unknown displacement increments $du$ and $dv$ obey to a linear system of algebraic equations, which can be expressed in the matrix form $\mathbf{K}_b d\boldsymbol{a} = d\boldsymbol{f}$, where the vector of unknowns $d\boldsymbol{a} = (du, dv)$. The elasto-geometric stiffness matrix $\mathbf{K}_b$ and the vector of known terms $d\boldsymbol{f} = (df_1, df_2)$ are

$$\mathbf{K}_b = \begin{bmatrix} 1 + \Lambda p_c \sec\vartheta\, k_x^h & -\Lambda p_c \sec\vartheta\, k_y^h \\ -\Lambda p_c \sec\vartheta\, k_x^v & 3\varrho_b^2 + \Lambda p_c \sec\vartheta\, k_y^v \end{bmatrix}, \qquad d\boldsymbol{f} = \begin{pmatrix} -h^\circ \Lambda p_c \sec\vartheta \\ (\nu^\circ - 2)\Lambda p_c \sec\vartheta - \frac{3}{8} p_b \end{pmatrix} \tag{101}$$

where the symmetry of the stiffness matrix $\mathbf{K}_b$ can be noticed, by recalling that $k_y^h = k_x^v$. The geometric $\Lambda$-dependent part of the stiffness matrix can be recognized. The unique solution $d\boldsymbol{a} = \mathbf{K}_b^{-1} d\boldsymbol{f}$ provides the incremental displacements

$$du = \frac{\left(k_y^v \Lambda p_c \sec\vartheta + 3\varrho_b^2\right) df_1 + k_y^h \Lambda p_b \sec\vartheta\, df_2}{3\varrho_b^2 + \Lambda p_c \sec\vartheta \left(\Lambda p_c K_{xy}^{hv} + 3k_x^h \varrho_b^2 + k_y^v\right)}, \qquad dv = \frac{k_x^v \Lambda p_c \sec\vartheta\, df_1 + \left(k_x^h \Lambda p_c \sec\vartheta + 1\right) df_2}{3\varrho_b^2 + \Lambda p_c \sec\vartheta \left(\Lambda p_c K_{xy}^{hv} + 3k_x^h \varrho_b^2 + k_y^v\right)} \tag{102}$$

where $K_{xy}^{hv} = \sec\vartheta(k_x^h k_y^v - k_y^h k_x^v)$. Solutions (102) are fully analytical (asymptotic) functions of the mechanical parameters. Indeed, the stiffness coefficients $k_x^h$, $k_y^h$, $k_x^v$, $k_y^v$ can be expressed as analytical functions of the mechanical parameters in the asymptotic form (89), while the $(h^\circ, \nu^\circ)$-dependent forces $df_1$ and $df_2$ can be expressed as analytical functions of the mechanical parameters by employing the asymptotic forms (29)-(31) and (32)-(34) of the reactions for the cable between fixed supports.

The fully analytical asymptotic solutions (102) can be compared with the exact numerical solutions, as can be achieved through the hybrid displacement-force method. From the qualitative viewpoint, the analytical asymptotic solutions (gray ruled wireframe surfaces in Fig. 9) are found to linearly approximate the nonlinear exact solutions for growing loads $p_b$, consistently with the expectations. From the quantitative viewpoint, the comparison shows that the linear approximation has naturally higher accuracy in the range of low beam loads. The approximation accuracy also degrades for lower values of the cable aspect ratios ($\Lambda \simeq 1$), which anticipate the nonlinear behavior, due to the early occurrence of the locking phenomenon. These remarks are also confirmed by the relative error $de_s = |(ds_{[6]} - s^*)/(\max(s^*) + s^*)|$ lower than $2 \times 10^{-1}$, which attains larger values for large loads and lower aspect ratios (see Fig. 9d).

## 5. Conclusions

In the first part of the paper, asymptotic descriptions of the catenary configuration assumed by inclined inextensible cables are determined, by means of a consistent perturbation method. Specifically, the perturbation scheme provides fully analytical solutions for the indeterminate static equilibrium problem that systematically – although asymptotically – satisfy the integral compatibility equation. This major achievement allows to circumvent the computational bottlenecks related to the numerical assessment of the horizontal component of the axial tension, playing the role of hyperstatic unknown. Indeed, the perturbation-based solutions have the form of fully analytical polynomial series – with terms of increasing order of smallness –, expressing all the static unknowns (configuration descriptors, internal forces, support reactions) as explicit parametric functions of the mechanical data (chord inclination and aspect ratio). As remarkable methodological point, the asymptotic polynomial solutions are not determinable by the direct series expansion of the exact catenary solutions, but require an indirect two-step strategy, consisting in stating and solving in closed form a linear differential system of *perturbation equilibrium equations* (first step) and, subsequently, a linear algebraic system of *perturbation compatibility equations* (second step). The outlined perturbation strategy can also be regarded as a generalizable methodological tool, whose technical principles could be systematically extended to search for analytical (asymptotically convergent) solutions of nonlinear static equilibrium problems related to statically indeterminate structures.

The accuracy of the asymptotic description for the exact catenary configuration is naturally limited, if a finite number of terms is considered in the polynomial series. Nonetheless, these limitations are compensated by the actual possibility to achieve the desired approximation accuracy by consistently extending the perturbation scheme to high orders. In this regard, very high-order results are presented and discussed from a mathematical and physical perspective. From the mathematical viewpoint, (i) the conditions for the existence of admissible solutions and for the consistency of the asymptotic approximation are introduced, (ii) the structural properties (symmetries, zeroes) of the series terms are recognized or demonstrated, (iii) the relative smallness (or greatness) of all the unknown quantities is assessed. Furthermore, parametric analyses are carried out to qualitatively discuss the perturbation solutions in the parameter space, as well as to quantitatively verify the growing approximation accuracy for increasing orders. From the mechanical viewpoint, the perturbation based solutions are found to provide proper mathematical support for some simplifying assumptions traditionally introduced in physical-mathematical models of shallow inclined cables.

In the second part of the paper, the geometric stiffness matrix governing the linearized relationship between boundary forces (or reactions) and support displacements of the inclined inextensible cables is considered. First, the exact catenary stiffness matrix is obtained, by analytically differentiating the implicit force-to-displacement relation stated by the integral compatibility condition. Therefore, the quasi-analytical catenary stiffness matrix, depending on the hyperstatic unknown (to be determined numerically) is asymptotically expressed in polynomial series – with terms of increasing order of smallness – as fully-analytical function of the mechanical parameters. From the methodological viewpoint, this achievement requires updating the two systems of perturbation equilibrium equations and perturbation compatibility equations, in order to account for displaceable supports. The key point is the valuable possibility to achieve explicit and high-order force-to-displacement relations, suited for analytical differentiation. From the mathematical viewpoint, the structural properties (symmetries, positiveness) of the series terms describing each stiffness coefficient are recognized. From the physical viewpoint, the relative orders of smallness (or greatness) of the dominant geometrical contributions to the cable stiffness are discussed, on the base of their mechanical interpretation. From the quantitative viewpoint, parametric analyses show how the perturbation based solutions approximate the stiffness coefficients with satisfying agreement in the parameter space even at the lower orders, whereas excellent agreement can be reached by increasing series orders.

From the application perspective, the availability of fully analytical – although asymptotically approximate – expression of the geometric stiffness matrix is a significant advancement for the model formulation and parametric design of complex cable nets or cable structures, according to the direct stiffness method. To exemplify, the prototypical case study concerning a cantilever cable-stayed beam is successfully analyzed to verify the accuracy of the analytical solutions provided by the perturbation strategy. Within the framework of the direct stiffness method, the high-order perturbation strategy provides highly accurate parametric solutions and – in the incremental formulation of the nonlinear quasi-static problem – does not require any numerical solution of the compatibility equations, which are automatically satisfied.

## Declaration of competing interest

The authors declare that they have no known competing financial interests or personal relationships that could have appeared to influence the work reported in this paper.

## Data availability

Data will be made available on request.

## Appendix A. Auxiliary quantities

### A.1. Configuration function

The coefficient characterizing the asymptotic expression $y_{[n]}(x)$ of the cable configuration function defined in equation (27) read (for the approximation errors $n \leq 6$)

$$
\begin{aligned}
&d_{10} = \tan\vartheta, && d_{11} = 4\delta_1 \sec\vartheta, && d_{12} = -4\delta_1 \sec\vartheta && \\
&d_{21} = \tfrac{16}{3}\delta_1^2 \tan\vartheta, && d_{22} = -16\delta_1^2 \tan\vartheta, && d_{23} = \tfrac{32}{3}\delta_1^2 \tan\vartheta, && \\
&d_{31} = \Delta_{31} \cos\vartheta, && d_{32} = -\Delta_{32} \sec\vartheta, && d_{33} = \tfrac{128}{3}\delta_1^3 \sec\vartheta, && d_{34} = -\tfrac{64}{3}\delta_1^3 \sec\vartheta \\
&d_{41} = \Delta_{41} \tan\vartheta, && d_{42} = -32\delta_1\delta_3 \tan\vartheta, && d_{43} = \Delta_{43} \tan\vartheta, && d_{44} = -\tfrac{256}{3}\delta_1^4 \tan\vartheta, \\
&d_{45} = \tfrac{512}{15}\delta_1^4 \tan\vartheta, && && && \\
&d_{51} = \Delta_{51} \cos\vartheta, && d_{52} = \Delta_{52} \sec\vartheta, && d_{53} = \Delta_{53} \cos\vartheta, && d_{54} = -\Delta_{54} \sec\vartheta \\
&d_{55} = \tfrac{2048}{15}\delta_1^5 \sec\vartheta, && d_{56} = -\tfrac{2048}{45}\delta_1^5 \sec\vartheta && && \\
&d_{61} = \Delta_{61} \tan\vartheta, && d_{62} = -\Delta_{62} \tan\vartheta, && d_{63} = \Delta_{63} \tan\vartheta, && d_{64} = -\tfrac{1024}{3}\delta_1^3\delta_3 \tan\vartheta \\
&d_{65} = \Delta_{65} \tan\vartheta, && d_{66} = -\tfrac{8192}{45}\delta_1^6 \tan\vartheta, && d_{67} = \tfrac{16384}{315}\delta_1^6 \tan\vartheta, && 
\end{aligned}
\tag{A.1}
$$

where the auxiliary quantities

$$
\begin{aligned}
&\Delta_{31} = \tfrac{32}{3}\delta_1^3 + 4\delta_3 \sec^2\vartheta && \Delta_{32} = \tfrac{32}{3}\delta_1^3\left(2+\cos^2\vartheta\right) + 4\delta_3 \\
&\Delta_{41} = -\tfrac{256}{45}\delta_1^4 + \tfrac{32}{3}\delta_1\delta_3 && \Delta_{43} = \tfrac{512}{9}\delta_1^4 + \tfrac{64}{3}\delta_1\delta_3 \\
&\Delta_{51} = \tfrac{128}{45}\delta_1^5 A_{51}(\vartheta) + 32\delta_1^2\delta_3 + 4\delta_5 \sec^2\vartheta && \Delta_{52} = \tfrac{128}{45}\delta_1^5 A_{52}(\vartheta) - 32\delta_1^2\delta_3\left(2+\cos^2\vartheta\right) - 4\delta_5 \\
&\Delta_{53} = \tfrac{1024}{9}\delta_1^5 + 128\delta_1^2\delta_3 \sec^2\vartheta && \Delta_{54} = \tfrac{512}{9}\delta_1^5\left(2+\cos^2\vartheta\right) + 64\delta_1^2\delta_3 \\
&\Delta_{61} = \tfrac{8192}{945}\delta_1^6 - \tfrac{1024}{45}\delta_1^3\delta_3 + \tfrac{32}{3}\delta_1\delta_5 + \tfrac{16}{3}\delta_3^2 && \Delta_{62} = 32\delta_1\delta_5 + 16\delta_3^2 \\
&\Delta_{63} = -\tfrac{8192}{135}\delta_1^6 + \tfrac{2048}{9}\delta_1^3\delta_3 + \tfrac{64}{3}\delta_1\delta_5 + \tfrac{32}{3}\delta_3^2 && \Delta_{65} = \tfrac{8192}{45}\delta_1^6 + \tfrac{2048}{15}\delta_1^3\delta_3
\end{aligned}
\tag{A.2}
$$

and the trigonometric quantities $A_{51}(\vartheta) = 8 - 5\cos^2\vartheta$ and $A_{52}(\vartheta) = 8 - 28\cos^2\vartheta + 5\cos^4\vartheta$ have been used.

### A.2. Asymptotic stiffness matrix

The independent coefficients $\gamma_{ij}^{\circ}$ of the vectors $\boldsymbol{\gamma}_i^{\circ}$ (for $i = 1,3,5$ and $j = 1,2$) defined in equation (74) read

$$
\begin{aligned}
&\gamma_{11}^{\circ} = \cos\vartheta && \gamma_{12}^{\circ} = \sin\vartheta \\
&\gamma_{31}^{\circ} = 15\cos^2\vartheta + 56 && \gamma_{32}^{\circ} = 3\left(5\cos^2\vartheta - 8\right)\tan\vartheta \\
&\gamma_{51}^{\circ} = 35\cos^2\vartheta\left(112 - 5\cos^2\vartheta\right) - 1408 && \gamma_{52}^{\circ} = 2176\tan\vartheta + 35\sin\vartheta\cos\vartheta\left(5\cos^2\vartheta + 48\right)
\end{aligned}
\tag{A.3}
$$

while the independent coefficients $\varphi_{ij}^{\circ}$ of vectors $\boldsymbol{\varphi}_i^{\circ}$ (for $i = 1,3,5$ and $j = 1,2$) defined in equation (75) are

$$
\begin{aligned}
&\varphi_{11}^{\circ} = 1 && \varphi_{12}^{\circ} = \tan\vartheta \\
&\varphi_{21}^{\circ} = 3 && \varphi_{22}^{\circ} = 2\tan\vartheta - \cot\vartheta \\
&\varphi_{31}^{\circ} = 15\cos^2\vartheta + 56 && \varphi_{32}^{\circ} = 3\left(5\cos^2\vartheta - 8\right)\tan\vartheta \\
&\varphi_{41}^{\circ} = 3\tan\vartheta && \varphi_{42}^{\circ} = -12\tan^2\vartheta - 5.
\end{aligned}
\tag{A.4}
$$

## Appendix B. Cable-stayed beam

### B.1. Governing equations

According to the definition of displacement and force variables illustrated in Fig. 8, the equations governing the static equilibrium of the inextensible cable and deformable flexible beam of the cable-stayed beam read

$$HY''(X)+w\left[1+\left(Y'(X)\right)^2\right]^{1/2}=0,\qquad EA_bU_b''(X_b)=0,\qquad EI_bV_b''''(X_b)+w_b=0, \tag{B.1}$$

where the apex indicates differentiation with respect to the abscissae $X\in[0,L]$ and $X_b\in[0,L]$ for the cable and the beam, respectively. The beam equations are equipped with the geometric boundary conditions

$$U_b(0)=0,\qquad V_b(0)=0,\qquad V_b'(0)=0 \tag{B.2}$$

and the mechanical (or natural) boundary conditions

$$EA_bU_b'(L)=-H,\qquad EI_bV_b''(L)=0,\qquad EI_bV_b'''(L)=wL_0-V, \tag{B.3}$$

which are sufficient to obtain solutions (91). The additional relations necessary to state and solve the kinematic compatibility conditions and the inextensibility condition (to determine the hyperstatic unknown $H$) are $Y(X_A)=Y_A$ at the cable support and $U_b(L)=X_B$ and $V_b(L)=-Y_B$ at the cable-beam node.

## References


[1] H. Irvine, Cable Structures, MIT Press Series in Structural Mechanics, MIT Press, 1981.
[2] G. Rega, Nonlinear vibrations of suspended cables - part I: modeling and analysis, Appl. Mech. Rev. 57 (2004) 443–478.
[3] G. Rega, Nonlinear vibrations of suspended cables - part II: deterministic phenomena, Appl. Mech. Rev. 57 (2004) 479–514.
[4] A. Luongo, D. Zulli, Mathematical Models of Beams and Cables, John Wiley & Sons, 2013.
[5] C. Truesdell, The influence of elasticity on analysis: the classic heritage, Bull. Am. Math. Soc. 9 (1983) 293–310.
[6] G. Conti, R. Paoletti, A. Trotta, The catenary in history and applications (La catenaria nella storia e nelle applicazioni), Sci. Philos. 5 (2017) 69–94.
[7] Q. Wu, K. Takahashi, S. Nakamura, Formulae for frequencies and modes of in-plane vibrations of small-sag inclined cables, J. Sound Vib. 279 (2005) 1155–1169.
[8] W. Lacarbonara, A. Paolone, F. Vestroni, Elastodynamics of nonshallow suspended cables: linear modal properties, J. Vib. Acoust. 129 (2007) 425–433.
[9] A. Mansour, O.B. Mekki, S. Montassar, G. Rega, Catenary-induced geometric nonlinearity effects on cable linear vibrations, J. Sound Vib. 413 (2018) 332–353.
[10] N. Srinil, G. Rega, S. Chucheepsakul, Three-dimensional non-linear coupling and dynamic tension in the large-amplitude free vibrations of arbitrarily sagged cables, J. Sound Vib. 269 (2004) 823–852.
[11] W. Lacarbonara, A. Paolone, F. Vestroni, Non-linear modal properties of non-shallow cables, Int. J. Non-Linear Mech. 42 (2007) 542–554.
[12] V. Gattulli, M. Lepidi, F. Potenza, U. Di Sabatino, Modal interactions in the nonlinear dynamics of a beam–cable–beam, Nonlinear Dyn. 96 (2019) 2547–2566.
[13] G. Rega, V. Settimi, S. Lenci, Chaos in one-dimensional structural mechanics, Nonlinear Dyn. 102 (2020) 785–834.
[14] D. Zulli, G. Piccardo, A. Luongo, On the nonlinear effects of the mean wind force on the galloping onset in shallow cables, Nonlinear Dyn. 103 (2021) 3127–3148.
[15] M. Lepidi, V. Gattulli, F. Vestroni, Static and dynamic response of elastic suspended cables with damage, Int. J. Solids Struct. 44 (2007) 8194–8212.
[16] M. Lepidi, V. Gattulli, Static and dynamic response of elastic suspended cables with thermal effects, Int. J. Solids Struct. 49 (2012) 1103–1116.
[17] V. Gattulli, R. Alaggio, F. Potenza, Analytical prediction and experimental validation for longitudinal control of cable oscillations, Int. J. Non-Linear Mech. 43 (2008) 36–52.
[18] A. Arena, E. Ottaviano, V. Gattulli, Dynamics of cable-driven parallel manipulators with variable length vibrating cables, Int. J. Non-Linear Mech. 151 (2023) 104382.
[19] M. Lepidi, V. Gattulli, F. Vestroni, Damage identification in elastic suspended cables through frequency measurement, J. Vib. Control 15 (2009) 867–896.
[20] C. Rinaldi, M. Lepidi, F. Potenza, V. Gattulli, Identification of cable tension through physical models and non-contact measurements, Mech. Syst. Signal Process. 205 (2023) 110867.
[21] A.H. Nayfeh, Perturbation Methods, Wiley-VCH Verlag GmbH, 2007.
[22] R.H. Rand, D. Armbruster, Perturbation Methods, Bifurcation Theory and Computer Algebra, vol. 65, Springer Science & Business Media, 2012.
[23] A. Luongo, On the use of the multiple scale method in solving difficult bifurcation problems, Math. Mech. Solids 22 (2017) 988–1004.
[24] M. Lepidi, Multi-parameter perturbation methods for the eigensolution sensitivity analysis of nearly-resonant non-defective multi-degree-of-freedom systems, J. Sound Vib. 332 (2013) 1011–1032.
[25] W. Lacarbonara, B. Carboni, G. Quaranta, Nonlinear normal modes for damage detection, Meccanica 51 (2016) 2629–2645.
[26] M. Lepidi, A. Bacigalupo, Parametric design of the band structure for lattice materials, Meccanica 53 (2018) 613–628.
[27] V. Denoël, E. Detournay, Multiple scales solution for a beam with a small bending stiffness, Struct. Eng. Mech. 136 (2010) 69–77.
[28] A. Luongo, D. Zulli, Statics of shallow inclined elastic cables under general vertical loads: a perturbation approach, Mathematics 6 (2018) 24.
[29] M. Triantafyllou, The dynamics of taut inclined cables, Q. J. Mech. Appl. Math. 37 (1984) 421–440.
[30] C. Lee, N.C. Perkins, Three-dimensional oscillations of suspended cables involving simultaneous internal resonances, Nonlinear Dyn. 8 (1995) 45–63.
[31] Y. Desai, Y.A. Shah, N. Popplewell, Perturbation-based finite element analyses of transmission line galloping, J. Sound Vib. 191 (1996) 469–489.
[32] P. Warnitchai, Y. Fujino, B.M. Pacheco, R. Agret, An experimental study on active tendon control of cable-stayed bridges, Earthq. Eng. Struct. Dyn. 22 (1993) 93–111.
[33] V. Gattulli, M. Pasca, F. Vestroni, Nonlinear oscillations of a nonresonant cable under in-plane excitation with a longitudinal control, Nonlinear Dyn. 14 (1997) 139–156.
[34] M. Lepidi, Catenary solutions for inextensible cables: a perturbation-based high-order approximation, in: V. Gattulli, M. Lepidi, L. Martinelli (Eds.), Dynamics and Aerodynamics of Cables - ISDAC 2023, Lecture Notes in Civil Engineering, vol. 399, Springer, 2024, pp. 229–239.
[35] A. Pevrot, A. Goulois, Analysis of cable structures, Comput. Struct. 10 (1979) 805–813.
[36] H. Jayaraman, W. Knudson, A curved element for the analysis of cable structures, Comput. Struct. 14 (1981) 325–333.
[37] L. Greco, N. Impollonia, M. Cuomo, A procedure for the static analysis of cable structures following elastic catenary theory, Int. J. Solids Struct. 51 (2014) 1521–1533.
[38] Y. Fujino, P. Warnitchai, B. Pacheco, An experimental and analytical study of autoparametric resonance in a 3dof model of cable-stayed-beam, Nonlinear Dyn. 4 (1993) 111–138.

[39] V. Gattulli, M. Morandini, A. Paolone, A parametric analytical model for non-linear dynamics in cable-stayed beam, Earthq. Eng. Struct. Dyn. 31 (2002) 1281–1300.
[40] V. Gattulli, M. Lepidi, Nonlinear interactions in the planar dynamics of cable-stayed beam, Int. J. Solids Struct. 40 (2003) 4729–4748.
[41] V. Gattulli, M. Lepidi, J.H. Macdonald, C.A. Taylor, One-to-two global-local interaction in a cable-stayed beam observed through analytical, finite element and experimental models, Int. J. Non-Linear Mech. 40 (2005) 571–588.
[42] V. Gattulli, A. Paolone, Planar motion of a cable-supported beam with feedback controlled actions, J. Intell. Mater. Syst. Struct. 8 (1997) 767–774.
[43] M. Magaña, J. Rodellar, Nonlinear decentralized active tendon control of cable-stayed bridges, J. Struct. Control. 5 (1998) 45–62.
[44] N. Luo, J. Rodellar, M. de la Sen, J. Vehí, Decentralized active control of a class of uncertain cable-stayed flexible structures, Int. J. Control 75 (2002) 285–296.
[45] Y. Xia, Y. Fujino, Auto-parametric vibration of a cable-stayed-beam structure under random excitation, J. Eng. Mech. 132 (2006) 279–286.